



Spinel compositions of mantle-hosted chromitite from the Eastern Anatolian ophiolite body, Turkey: Implications for deep and shallow magmatic processes

Kurtuluş Günay ^{a,*}, Ali Rıza Çolakoğlu ^b

^a General Directorate of Mineral Research and Exploration, Department of Mineral Research and Exploration, Ankara, Turkey

^b Geological Engineering Department, Yüzüncü Yıl University, Van, Turkey



ARTICLE INFO

Article history:

Received 2 July 2015

Received in revised form 16 October 2015

Accepted 18 October 2015

Available online 23 October 2015

Keywords:

Chromite

PGE

Magma processes

Ophiolite

Eastern Turkey

ABSTRACT

The Eastern Anatolian Accretionary Complex includes several ophiolitic megablocks and/or tectonic slivers within a 150–180 km long east–west trending complex formed during the Late Cretaceous–Tertiary in Eastern Turkey. The Alabayır, Mollatopuz, Yukaribalçıklı and Mehmetalan ophiolites are megablocks or tectonic slivers containing locally massive, nodular or schlieren banded chromitite layers. These podiform chromitites formed in mantle sequences and are classified as high-Cr chromitites ($\text{Cr} \#$ 0.63–0.88; $\text{Mg} \#$ 0.50–0.64; 0.01–0.5 wt.% TiO_2 ; 5.7–18.8 wt.% Al_2O_3). Calculated parental melt compositions of these chromitites indicate boninite magma characteristics (8.2–13.4 wt.% Al_2O_3 ; 0.64–1.50 FeO/MgO). The PGE patterns also support the view that they crystallized from a boninitic melt. The total PGE contents of chromitites vary between 79 and 390 ppb. Pd/Ir ratios of chromitites vary from 0.07 to 0.28 and are consistent with an IPGE fractionated nature. The examined chromitites were divided into two groups in terms of their mineral chemistry (Group-I: Alabayır, Mollatopuz, Yukaribalçıklı and Mehmetalan-I chromitites; Group-II: Mehmetalan-II chromitites). Mineral chemistry of these chromitites and their parental melt composition indicate that Group-I chromitites were probably formed at shallow mantle depths and that Group-II chromitites formed in deeper parts of the mantle. Mineral chemistry of these Eastern Anatolia high-Cr chromitites indicate that they formed not only in the deeper mantle but also in shallower parts of the MOHO transition zone.

© 2015 Elsevier B.V. All rights reserved.

1. Introduction

Turkish ophiolites represent the remnants of Tethyan Ophiolite Belt in the Anatolian segment of the Alpine–Himalayan Orogen. These ophiolites are found as tectonic complexes associated with E–W trending tectonic belts such as the Pontides, Anatolides, Taurides and the Border folds (Ketin, 1983; Okay and Tüysüz, 1999). The investigated chromitite zone is located in the Tethyan ophiolite belt, which extends from Spain to the Himalayas, and is characterized by podiform chromitite. Most of the Alpine–Himalayan Belt chromitites are podiform-type and occur in the mantle sequence of ophiolite complexes. The formation of podiform chromitite deposits has been discussed for many decades (e.g. Thayer, 1964, 1969; Dickey, 1975; Lago et al., 1982; Paktunc, 1990; Prichard and Lord, 1990; Kelemen et al., 1992; Leblanc and Nicolas, 1992; Zhou et al., 1994, 1998; Arai et al., 2004). Chrome spinel and platinum group element (PGE) geochemistry of ophiolitic chromitites provides important data about the petrological nature of the mantle sources and geodynamic emplacement of the chromitites (Melcher et al., 1997; Zhou et al., 1998; Proenza et al., 1999, 2004; Arai et al., 2006; Rollinson, 2008; Arai et al., 2011; Pal,

2011; Uysal et al., 2012). Recently most authors have agreed that ophiolitic chromites formed in the mantle section of ophiolites in Supra-subduction Zone (SSZ) environments during melt–rock reaction and/or melt–melt interaction (e.g. Dick and Bullen, 1984; Zhou and Robinson, 1997; Arai, 1997; Ballhaus, 1998; Zhou et al., 1994, 1998; Melcher et al., 1997, 1999; Proenza et al., 2004; Uysal et al., 2005, 2007a, 2007b; González-Jiménez et al., 2011; Zaccarini et al., 2011). In addition, stratigraphic placement of chromitites found within the mantle-oceanic lithosphere and their effect on characteristics of chromite formation are controversial. The basic consensus of these studies is that high-Cr chromitites ($\text{Cr} \# > 60$) are located in deep sections of the mantle, with high-Al chromitites ($\text{Cr} \# < 60$) located in the shallow sections of the mantle toward the petrologic MOHO (Rammlmair et al., 1987; Leblanc and Nicolas, 1992; Rollinson, 2008; Zaccarini et al., 2011; Dönmez et al., 2014).

Podiform chromitites may have been an important source for economic concentrations of PGE, with enrichment particularly of Ru, Os and Ir (IPGE group) (e.g. Economou-Eliopoulos, 1996; Melcher et al., 1997). Remnants of the Tethyan oceanic lithosphere mainly occur in Turkey as dismembered ophiolitic bodies, which are generally tectonically complex (Fig. 1A). There are many debates regarding the number and location of Turkish suture zones. One of the discussions

* Corresponding author.

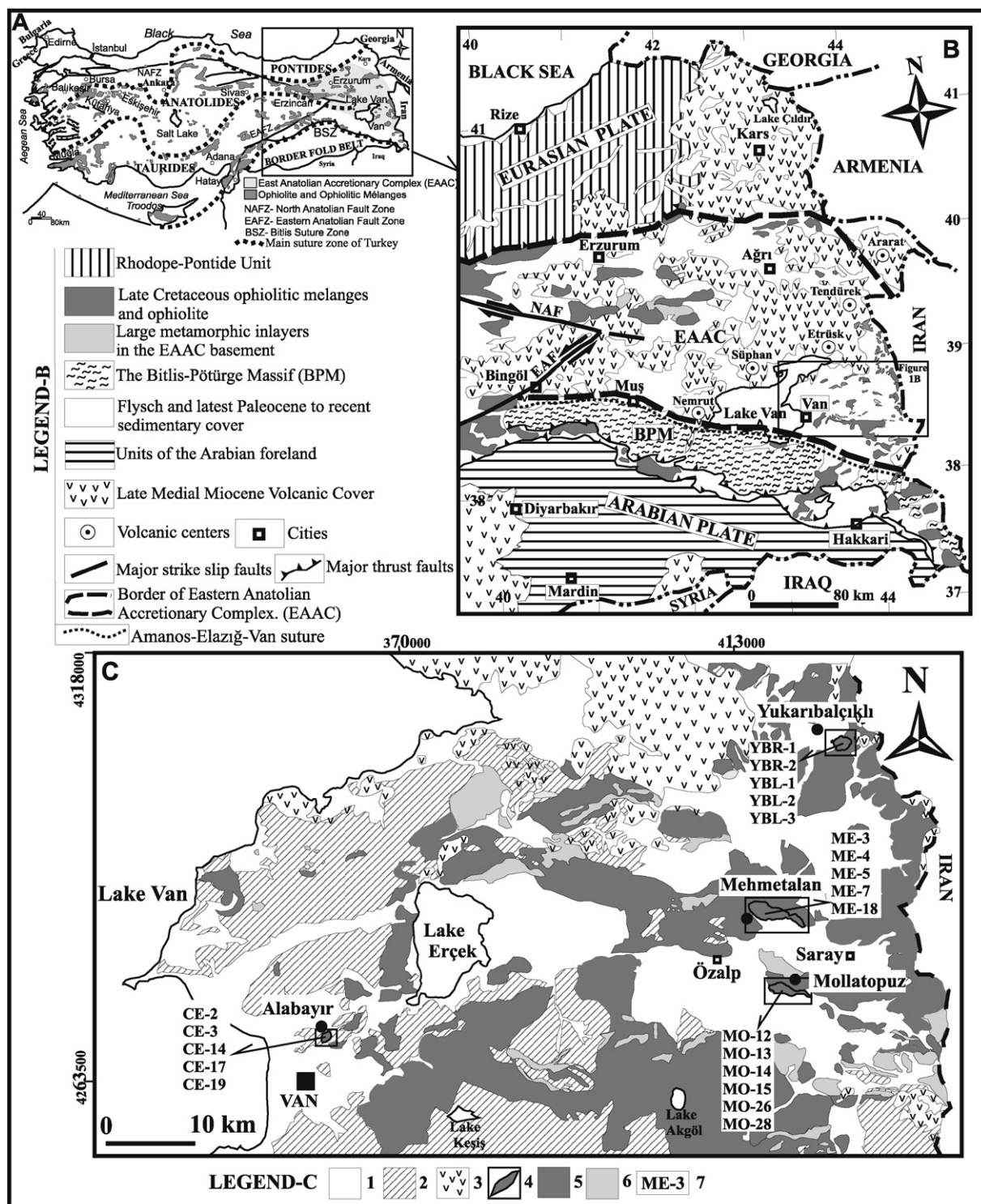


Fig. 1. 1A) Distribution of ophiolites in Turkey (Şenel and Ercan, 2002; Okay and Tüysüz, 1999) 1B) Simplified geological map of the Eastern Anatolia region modified from Keskin (2005). 1C. Geological map of eastern Lake Van modified from Şenel and Ercan (2002), and showing sampling locations of chromitite samples for PGE geochemistry and measured chromite compositions (Legend C: 1 – Pliocene-Quaternary fluvial sediment rocks, 2 – Paleocene-Miocene sediment rocks, 3 – Late Medial Miocene to recent collisional volcanics, 4 – Mehmetalan, Mollatopuz, Yukarıbalçıklı and Alabayır ophiolites, 5 – Upper Cretaceous-Paleogene ophiolitic melange and related rocks, 6 – Paleozoic metamorphic rocks, and 7 – sample locations).

involves the number of branches southeast of the Neotethys sutures. There are three different models. The first model includes three sutures as suggested by Şengör (1984) (Assyride, Çüngüs and Maden sutures). The second model suggests two suture zones south and north of Bitlis-Pötürge massif (Fig. 1B) and is mainly accepted by Oberhaensli et al. (2012); Parlak et al. (2012) and Karaoğlan et al. (2013, 2014). The last model has been suggested by Göncüoğlu et al. (1997) and

Çolakoğlu et al. (2014) purports that only one branch with a suture located north of the Bitlis-Pötürge massif, called the Amanos-Elazığ-Van suture (Fig. 1B).

The ophiolite belts of Turkey host economically important chromitite deposits within mantle peridotites. The most important ones are located in Muğla, Erzincan-Sivas, Elazığ, Bursa-Eskişehir, Adana-Mersin and Hatay-Kahramanmaraş areas (Fig. 1A). Chromitite deposits of Turkey

have been documented by several authors in the last decade in terms of PGE enrichment, mineral phases and their chromite compositions (e.g. Uçurum et al., 2000, 2006; Uysal et al., 2005, 2007a, 2007b, 2009a, 2009b; Başpinar, 2006; Akbulut et al., 2010). Podiform chromite deposits have higher enrichment of Ru–Os–Ir than Rh–Pt–Pd. However, Turkish podiform chromitites have low PGE content generally, with an average of 200–300 ppb. But local Pt and Pd enrichment zones are known and reported in Harmancık Muğla (Uçurum et al., 2006) and Kahramanmaraş–Berit ophiolite (Kozlu et al., 2014). The present study reports the first systematic investigation of chromite composition and PGE data from four different chromitite deposits hosted in the Eastern Anatolian Accretionary Complex. The aim of this paper is to describe genetic relationships, nature of the parental melt and tectonic settings of the chromitites within the southeast Neotethyan oceanic basin.

2. Geological background

As part of the Alpine–Himalayan mountain system, the topography of the Eastern Anatolian region of Turkey has a mean elevation of approximately 2 km (Şengör and Kidd, 1979). It has attained this height since the mid-Miocene–Serravallian stage (Şengör et al., 2003; Dewey et al., 1986). New apatite fission-track data are interpreted to indicate that uplift occurred between 18 and 13 Ma and rapidly increased at ~12 Ma (Okay et al., 2010). The geological setting of the study area is mainly composed of Paleozoic metamorphic rocks, Upper Cretaceous ophiolitic mélange, Oligocene–Miocene sediments, Middle Miocene to Quaternary aged volcanics and recent sediments (Fig. 1B). In this sequence, the oldest metamorphic units have been interpreted as parts of the Anatolide–Tauride microcontinent (e.g. Göncüoglu et al., 1997; Okay and Tüysüz, 1999). In tectonic classifications, Eastern Anatolia was initially included in the Eastern Anatolian Accretionary Complex (Fig. 1B, EAAC, Şengör et al., 2003), which formed as a large subduction–accretion complex during the northward subduction of the Neotethyan oceanic lithosphere beneath the Eurasian continent during the Late Cretaceous–Oligocene (Şengör et al., 2003; Keskin, 2005; Şengör et al., 2008). Within this zone, mafic–ultramafic associations representing parts of a dismembered ophiolite complex are abundant east of the Lake Van area. The Alabayır, Mehmetalan and Mollatopuz ophiolitic bodies are parallel to the Zagros Thrust Zone, except the Yukarıbaçıklı ophiolitic bodies (Fig. 1C). These ophiolitic slices are generally represented by peridotite (harzburgite), gabbro, serpentinite and mafic dykes. The greater part of the area was covered by thick volcanic units during the late Miocene–Pliocene period (Innocenti et al., 1976), but there is some debate about the initiation of volcanic activity in the region (e.g. Yılmaz et al., 1987; Şengör et al., 2008; Çolakoglu and Arehart, 2010). Beneath the volcanics, the EAAC consists of flysch units. The flysch deposits are younger from north to south; indicating that the corresponding basins became shallower from Cretaceous to Oligocene (Şengör and Yılmaz, 1981; Acarlar et al., 1991; Şengör et al., 2003).

Geology of the Mehmetalan, Yukarıbaçıklı, Mollatopuz and Alabayır ophiolites and geochemistry of diabase dykes that crosscut all the ophiolitic units were studied by Günay (2011), Günay et al. (2012), Çolakoglu et al. (2012). Isolated diabase dykes in the Mehmetalan and Mollatopuz ophiolites exhibit SSZ/E-MORB character. There is a lack of isolated diabase dykes from the Yukarıbaçıklı ophiolites, however, isolated diabase dykes that cross cutting the Alabayır ophiolite exhibit OIB-like (ocean island basalts) affinity (Günay, 2011; Çolakoglu et al., 2012). Diabase dykes seen in the Alabayır area cut both ophiolite and chromitite. Çolakoglu et al. (2012) divided the geochemistry of diabase dykes into three different groups. They are: i) supra-subduction zone (SSZ) type, which is characterized by marked Nb-anomaly and normal mid-ocean ridge basalt (N-MORB) like HFSE distribution, ii) enriched MORB (E-MORB) type, showing some degree of enrichment relative to N-MORB, and iii) oceanic-island basalt (OIB) type with characteristic convex-shaped trace element patterns, coupled with fractionated REE distribution.

Chromite deposits in the area have been grouped into four geographically distinct areas: 1) Mehmetalan chromitites (ME), 2) Yukarıbaçıklı chromitites (YB), 3) Mollatopuz chromitites (MO), and 4) Alabayır chromitites (CE). The general geological characteristics of this area are summarized in Table 1. Nodular type chromitites are only observed in the Mehmetalan area. Nodules of chromite range from 0.3–1.5 cm and are hosted within an olivine-rich matrix. The nodular bands have thicknesses of 50 cm and can be traced over distances of 25 m. Schlieren banded chromitites were seen in all distinct areas. Schlieren banded chromitites typically occur as rhythmic layers with olivine-rich bands having thicknesses of 2 to 5 m and extending over lengths of 5 to 20 m. Serpentinized olivine matrix increases gradually from massive to schlieren banded chromitites. Massive chromitites and host peridotites are highly deformed and exhibit shear effects and various boudin shapes. Most of the chromitite bodies range from 5 to 20 m long, 2 to 5 m wide and 0.5 to 2 m thick.

Chromitites are typically and mostly observed as lens shaped – massive and nodular, but are also partly seen in tabular and schlieren form. Most of the chromitites are observed to be parallel to the peridotite foliation. However, massive chromitites and host peridotites are highly deformed and have shear effects and boudin shape.

3. Analytical methods

A total of 8 chromitite samples were selected from the Alabayır, Mehmetalan, Mollatopuz and Yukarıbaçıklı area for PGE geochemistry. Chromitite samples were analyzed for six PGE elements and Au using a nickel sulfide fire-assay pre-concentration method followed by ICP–MS at the Perth-Genalysis Laboratory, Western Australia. Detection limits were 2 ppb for Os, Ir, Ru, Pt and Pd, 1 ppb for Rh, and 5 ppb for Au. AMIS0014 Certified Reference Materials were used to ensure accuracy. Electron microprobe quantitative analyses of chromium spinel were investigated in WDS mode using a Superprobe Jeol JXA 8200 (Laboratory Eugen F. Stumpfl, University of Leoben, Austria) operating with 15 kV accelerating voltage and 10 nA beam current. The beam diameter was approximately 1 μm. The proportion of trivalent iron in chromian spinel was calculated assuming the ideal stoichiometry. Selected electron microprobe analysis results (wt.%) and atomic proportions of chromites are presented in Table 2. Minimum and maximum main oxide values of the chromite chemistry results are shown in Table 3. The PGE and Au data are presented in Table 4.

4. Petrography

Forty thin sections and 60 polished samples were prepared from both chromitite and the host rocks. The petrographic features of chromitites and host-rocks were examined under a Leica microscope. Ultramafic rocks associated with chromitites in the study area are highly serpentinized. The porphyro-granoblastic texture in harzburgites has been replaced by mesh textures due to serpentinization. The relict porphyroclastic orthopyroxenes in harzburgites have plastic deformation characteristics like rotation and kink bands. The host-rocks are dunite and harzburgite, comprising 4–10% and <4% chromite respectively. Massive chromite pods have sharp contacts with host-rocks (Fig. 2A), while nodular and schlieren-banded chromitites are enveloped by dunite (Fig. 2B–C). Boudin shape chromitites are common in the shear zones (Fig. 2D). Serpentintized dunites display mesh texture and some relict olivine is still preserved. Serpentintized harzburgites are mainly composed of primary olivine, orthopyroxene, clinopyroxene along with secondary hornblende, talc, calcite, epidote and opaques (Fig. 2E). Orthopyroxene shows kink bands in porphyro-granoblastic textured harzburgites (Fig. 2F–G). Chromite grains show high reflectivity, and dark to pale gray colors are typical in polished sections (Fig. 2H). There are optical color differences between the unaltered centers and the altered edges of the chromite grains. The alteration observed at the edges and along cracks–fractures in the chromite grains has a light

Table 1

Geological characteristics of Eastern Anatolia ophiolites (Günay, 2011; Çolakoğlu et al., 2012).

Location	Alabayır area	Mollatopuz area	Yukarıbalıklı area	Mehmetalan area
Field description	The ophiolitic body occurs as a tectonic slice with tectonic contacts Upper Paleocene–Early Miocene sediments	The ophiolitic body occurs as a tectonic sliver within the Lutetian–Oligocene sediments	The ophiolitic body occurs as a tectonic slice with tectonic contacts Upper Paleocene–Early Miocene sediments	The ophiolitic body occurs as a tectonic sliver within the Lutetian–Oligocene sediments
Ophiolite description	Ophiolitic melângé	Ophiolitic melângé	Ophiolitic melângé	Ophiolitic melângé
Rock type	The ophiolitic body is represented serpentized harzburgite, serpentinite, dunite, pyroxenite dykes. The partly preserved mafic cumulate units consist of olivine gabbro, troctolite and layered gabbro. The ultramafic and mafic units of Alabayır ophiolite are cut by isolated diabase dykes.	The dominating rock-unit is ultramafic tectonites (serpentized harzburgite, serpentinite, dunite) with rare mafic–ultramafic cumulates (layered gabbro, olivine gabbro, pegmatitic gabbro, pyroxenite–dunite intercalation). The cumulates are cut by pyroxenite dykes. The ophiolitic bodies are cut by isolated diabase dykes.	The ophiolitic body is represented serpentinite and dunite. Ultramafic cumulates consist of wherlite and pyroxenite–dunite intercalation. The partly preserved mafic cumulate units consist of olivine gabbro, troctolite and layered gabbro.	The dominating rock-unit is ultramafic tectonites (serpentized harzburgite, serpentinite, dunite) with rare mafic–ultramafic cumulates (layered gabbro, olivine gabbro, pegmatitic gabbro, pyroxenite–dunite intercalation). The cumulates are cut by pyroxenite dykes. The ophiolitic bodies are cut by isolated diabase dykes.
Geochemistry of dykes	Oceanic-island basalt (OIB) type with characteristic hump-backed trace element patterns	Supra-subduction zone (SSZ) type, which is characterized by marked Nb-anomaly and normal mid-ocean ridge basalt (N-MORB) like HFSE distribution. Enriched MORB (E-MORB) type, showing some degree of enrichment relative to N-MORB	E-MORB-type sample Ar/Ar plateau age of 105.4 ± 1.1 Ma, whereas another sample with SSZ-characteristics sample is dated with 92.0 ± 0.9 Ma	E-MORB-type sample Ar/Ar plateau age of 105.4 ± 1.1 Ma, whereas another sample with SSZ-characteristics sample is dated with 92.0 ± 0.9 Ma
Age of dykes	Ar/Ar whole rock dating of OIB-like from the Alabayır dyke yielded a plateau age of 87.7 ± 1.0 Ma			
Type of chromitites	Lens shaped – massive and partly seen in tabular and schlieren form	Lens shaped – massive and partly seen in tabular and schlieren form	Lens shaped – massive and partly seen in tabular and schlieren form	Lens shaped – massive and nodular, partly seen in tabular and schlieren form

gray color, while the dark-gray center sections of the chromite grains have not been affected by alteration (Fig. 2I). Massive chromitites, nodular and schlieren-banded chromitites have modal chromite contents of 75% (by vol.), 30–50% (by vol.) and 20–40% (by vol.), respectively. Chromite grains range in size from 0.5–3 mm in massive chromitite, 0.2–1.5 mm in nodular chromitite and 0.1–2 mm in schlieren-banded chromitites. 6–Massive chromitites show fractured-sheared and containing highly annealed chromite grains textures (Fig. 2J). Schlieren-banded type chromitites show cumulate textures (Fig. 2K). Nodular chromite has pull-apart cracks and cataclastic textures (Fig. 2L).

In the study area, the ultramafic–mafic rocks occur as tectonic slices above the harzburgites consist of pyroxenite, dunite (Fig. 3A), pyroxenite dykes, wherlite, troctolite, olivine gabbro, layered gabbro, pegmatitic gabbro dykes and diabase dykes. In the pyroxenites, clinopyroxene + orthopyroxene + olivine + serpentine are observed in the paragenesis with mesocumulate textures. Exsolution lamellae and banded textures are frequently seen in the clinopyroxenes. There are occasional hypersthene transformations in the exsolution lamellae (Fig. 3B). In dunites relict olivine minerals occur in a matrix with advanced serpentization (Fig. 3C). Wherlites exhibit cumulate texture in thin section. The main paragenesis observed in these sections is clinopyroxene + olivine \pm orthopyroxene + serpentine minerals, cumulus pyroxene crystals with intercumulus olivine crystals (Fig. 3D). Olivine gabbro and troctolite has hypidiomorphic granular texture with partially serpentized olivine, clinopyroxene and generally sericitized plagioclase paragenesis (Fig. 3E–F). Pegmatitic gabbros are generally formed of 3–5 cm pyroxene, hornblende and plagioclase crystals (Fig. 3G). Cumulate gabbros are frequently cut by thin pegmatitic gabbro veins. Isolated diabase dykes cutting ultramafic rocks typically exhibit ophitic texture and are partially rodingitized due to calcium metasomatism. The general mineral paragenesis in these dykes consists of orthopyroxenes, clinopyroxenes, plagioclase, hydrogrossular, phlogopite, chlorite, epidote, apatite, calcite and opaque minerals (Fig. 3 H–I).

5. Chromite geochemistry

For mineral chemistry surveys, an analyzed point was selected from unaltered chromite. Chromites were determined to be magnesio-chromite with $\text{Cr} \# > 0.5$ and $\text{Mg} \# \geq 0.5$. The mineral chemistry results of chromites from all the chromitites display similar values, but only the Mehmetalan chromitite sample results have two distinguishable groups. For this reason, chromite mineral chemistry data is divided into two groups. The first group of chromitites (Group-I: Alabayır, Mollatopuz, Yukarıbalıklı and Mehmetalan-II chromitites) has values of $47.4\text{--}56.9 \text{ Cr}_2\text{O}_3 \text{ wt.\%}$, $12.3\text{--}18.7 \text{ Al}_2\text{O}_3 \text{ wt.\%}$ and $0.06\text{--}0.55 \text{ TiO}_2 \text{ wt.\%}$ (Table 2). The second group (Group-II: Mehmetalan-II chromitites) of chromitites has values of $58.4\text{--}66.0 \text{ Cr}_2\text{O}_3 \text{ wt.\%}$, $5.8\text{--}7.9 \text{ Al}_2\text{O}_3 \text{ wt.\%}$ and $0.01\text{--}0.24 \text{ TiO}_2 \text{ wt.\%}$ (Table 2). While Cr_2O_3 contents increase from Alabayır to Memetalan II chromitites, the TiO_2 contents decrease as shown in Table 3.

Mehmetalan-II chromitites display the lowest Al_2O_3 and TiO_2 values and the highest Cr_2O_3 contents. Al_2O_3 versus Cr_2O_3 diagram shows that all the chromitite samples fall within the podiform chromitite field (Fig. 4A). $\text{Cr} \#$ and $\text{Mg} \#$ values of the chromitite samples ($\text{Cr} \# = [100 \text{ Cr}/(\text{Cr} + \text{Al})]$ and $\text{Mg} \# = [100 \text{ Mg}/(\text{Mg} + \text{Fe})]$) range between 0.63–0.75 and 0.50–0.64 in Group-I and 0.83–0.88 and 0.50–0.55 in Group-II. In Group-I chromitites, $\text{Cr} \#$ versus TiO_2 content displays a negative correlation (Fig. 4B). All the chromitites are referred to as high Cr–chromite due to their high $\text{Cr} \# > 0.6$. The $\text{Cr} \#$ versus $\text{Mg} \#$ diagram shows that all the chromitite samples fall in the supra-subduction zone peridotite field as shown in Fig. 4C.

6. PGE geochemistry

Total PGE concentrations in the analyzed chromitites vary from 79 to 390 ppb while the Au values are lower than the detection limit. The chondrite-normalized PGE patterns of the chromitites are illustrated in Fig. 5. The results are characterized by enrichment in IPGE (Os, Ir,

Table 2

Selected electron microprobe composition (wt.%) and atomic proportions of chromites from Eastern Anatolia chromitites.

Group I chromitites															Group II chromitites					
wt.%	CE-2	CE-3	CE-14	CE-17	CE-19	MO-12	MO-13	MO-14	MO-15	MO-28	YBR-1	YBR-2	YBL-1	YBL-2	YBL-3	ME-7	ME-18	ME-3	ME-4	ME-5
TiO ₂	0.45	0.47	0.42	0.55	0.43	0.38	0.33	0.40	0.42	0.33	0.20	0.15	0.24	0.27	0.24	0.12	0.13	0.04	0.03	0.06
V ₂ O ₅	0.16	0.19	0.19	0.17	0.15	0.11	0.13	0.09	0.10	0.12	0.16	0.09	0.14	0.20	0.14	0.11	0.12	0.24	0.28	0.26
Al ₂ O ₃	17.01	16.65	16.39	15.03	16.40	15.32	16.33	13.38	14.33	16.14	14.78	14.63	15.39	16.39	16.63	14.93	13.68	5.79	6.22	7.06
Cr ₂ O ₃	52.43	51.31	51.50	52.87	53.18	52.04	52.25	54.60	54.23	51.46	55.50	54.48	54.26	53.13	53.58	54.86	56.43	64.99	64.65	63.31
FeO	15.97	16.11	16.00	15.98	15.83	15.50	15.90	16.36	16.75	16.51	15.61	15.16	15.96	14.80	15.29	15.54	15.65	17.10	17.08	17.22
Fe ₂ O ₃	0.84	2.06	2.32	1.99	1.22	3.29	1.71	2.66	3.10	2.57	1.03	1.71	1.08	1.11	0.17	1.02	0.79	1.27	0.65	1.57
MgO	12.40	12.26	12.19	12.07	12.50	12.36	12.08	11.67	11.82	11.76	12.34	12.26	12.05	12.82	12.47	12.10	11.89	10.44	10.33	10.48
NiO	0.09	0.06	0.17	0.17	0.07	0.19	0.20	0.12	0.13	0.09	0.05	0.12	0.12	0.18	0.20	0.10	0.11	0.06	0.05	0.12
ZnO	0.02	0.01	0.08	0.06	0.05	0.00	0.14	0.01	0.08	0.08	0.04	0.11	0.06	0.12	0.04	0.10	0.14	0.01	0.16	0.07
Total	99.39	99.13	99.25	98.90	99.86	99.24	99.09	99.32	100.98	99.05	99.77	98.73	99.31	99.02	98.76	98.92	98.96	99.95	99.44	100.16
At. Prop.																				
Cr	1.31	1.29	1.30	1.35	1.33	1.32	1.32	1.40	1.36	1.31	1.40	1.39	1.37	1.34	1.35	1.40	1.45	1.73	1.72	1.67
Ti	0.01	0.01	0.01	0.01	0.01	0.01	0.01	0.01	0.01	0.005	0.004	0.004	0.006	0.006	0.006	0.003	0.003	0.001	0.001	0.001
V	0.003	0.004	0.004	0.004	0.003	0.002	0.003	0.002	0.002	0.002	0.003	0.002	0.003	0.004	0.003	0.002	0.003	0.01	0.01	0.01
Al	0.64	0.63	0.62	0.57	0.61	0.58	0.62	0.51	0.54	0.61	0.56	0.56	0.58	0.61	0.63	0.57	0.52	0.23	0.25	0.28
Fe ³⁺	0.02	0.05	0.06	0.05	0.03	0.08	0.04	0.06	0.07	0.06	0.02	0.04	0.03	0.03	0.004	0.02	0.02	0.03	0.02	0.04
Fe ²⁺	0.42	0.43	0.43	0.43	0.42	0.42	0.43	0.44	0.45	0.44	0.42	0.41	0.43	0.39	0.41	0.42	0.42	0.48	0.48	0.48
Mg	0.59	0.58	0.58	0.58	0.59	0.59	0.58	0.56	0.56	0.56	0.59	0.59	0.58	0.61	0.59	0.58	0.57	0.52	0.52	0.52
Ni	0.002	0.002	0.004	0.004	0.002	0.005	0.005	0.003	0.003	0.002	0.001	0.003	0.003	0.004	0.01	0.002	0.003	0.001	0.001	0.003
Zn	0.001	0.0001	0.002	0.002	0.001	0.000	0.003	0.0003	0.002	0.002	0.001	0.003	0.001	0.003	0.001	0.002	0.003	0.0001	0.004	0.002
Total cat.	3.00	3.00	3.00	3.00	3.00	3.00	3.00	3.00	3.00	3.00	3.00	3.00	3.00	3.00	3.00	3.00	3.00	3.00	3.00	3.00
Mg#	58	58	58	57	58	59	58	56	56	56	58	59	57	61	59	58	58	52	52	52
Cr#	67	67	68	70	69	69	68	73	72	68	72	71	70	68	68	71	73	88	87	86
Al#	0.32	0.32	0.31	0.29	0.31	0.29	0.31	0.26	0.27	0.31	0.28	0.28	0.29	0.31	0.32	0.29	0.26	0.12	0.14	
Fe ³⁺ #	0.01	0.03	0.03	0.02	0.01	0.04	0.02	0.03	0.04	0.03	0.01	0.02	0.01	0.01	0.00	0.01	0.02	0.01	0.02	
Fe ²⁺ /Fe ³⁺	21.05	8.71	7.68	8.93	14.40	5.24	10.31	6.84	6.00	7.15	16.77	9.88	16.42	14.85	101.84	16.87	22.09	14.97	29.41	12.17
(FeO/MgO) _{spinel}	1.29	1.31	1.31	1.32	1.27	1.25	1.32	1.40	1.42	1.40	1.27	1.24	1.32	1.15	1.23	1.28	1.32	1.64	1.65	1.64
(FeO/MgO) _{melt}	0.84	0.85	0.85	0.86	0.83	0.80	0.86	0.90	0.91	0.91	0.82	0.80	0.86	0.75	0.81	0.84	0.86	1.03	1.05	1.04
(Al ₂ O ₃) _{melt}	13.68	13.57	13.49	13.04	13.49	13.14	13.47	12.43	12.79	13.41	12.95	12.89	13.16	13.49	13.57	13.00	12.54	8.05	8.43	9.09
(TiO ₂) _{melt}	0.58	0.60	0.55	0.69	0.55	0.51	0.44	0.53	0.55	0.45	0.30	0.25	0.35	0.38	0.35	0.22	0.23	0.13	0.13	0.15

Table 3

Microprobe analysis of chrome spinel min–max wt.% values.

Group-I chromitites					Group-II chromitites
wt.%	Alabayır	Mollatopuz	Yukarıbalıkçılı	Mehmetalan-I	Mehmetalan-II
Cr ₂ O ₃	47.58–53.47	47.35–54.60	49.70–54.43	51.53–56.89	58.43–65.96
Al ₂ O ₃	15.03–18.86	13.20–17.23	12.33–17.83	13.32–16.54	5.79–7.92
MgO	11.89–13.47	11.22–12.93	10.12–13.81	10.81–13.61	10.03–11.10
FeO	14.25–16.72	15.04–17.23	13.78–17.93	13.79–17.64	15.52–17.96
Fe ₂ O ₃	0.74–4.21	0.00–5.61	0.00–3.45	0.00–3.67	0.00–2.66
TiO ₂	0.36–0.55	0.29–0.49	0.14–0.36	0.06–0.24	0.01–0.24
Mg#	56–62	53–60	50–64	56–63	50–55
Cr#	63–70	64–73	65–75	68–73	83–88

Ru) relative to PPGE (Rh, Pt, Pd) with the (IPGE)/(PPGE) ratio in the Van area chromitites varying between 1.95 to 6.15. PGE data show an enriched IPGE pattern with positive Ru and negative Pt anomaly. However, YB numbered samples show distinct concentrations of Ru and slightly positive concentrations of Os and Ir. Only the Mehmetalan samples (ME 3–4) have higher Pt values (24–27 ppb) compared to the rest of the samples which range from 3 to 15 ppb.

7. Discussion

7.1. Parental melt composition of chromitite

The composition of the chromite is a proxy for the genesis of rocks in different geodynamical environments (Dick and Bullen, 1984; Zhou et al., 1998; Kamenetsky et al., 2001; Arai et al., 2004, 2006, 2011; Garuti et al., 2007; Rollinson, 2008; González-Jiménez et al., 2009, 2011; Pal, 2011). According to recent research, it has been accepted that chromitites form during melt–rock reaction and/or melt–melt interaction in the supra-subduction zone (SSZ) environment (Zhou and Robinson, 1994; Zhou et al., 1998; Melcher et al., 1999; Kamenetsky et al., 2001; Uysal et al., 2005, 2009a, 2009b; González-Jiménez et al., 2011; Zaccarini et al., 2011). Furthermore, there is a continuing debate (Rollinson, 2008; Arai et al., 2011; González-Jiménez et al., 2011; Pal, 2011; Zaccarini et al., 2011) on the main melting processes of chromitite occurrences with different chemical compositions (high-Cr and low-Ti, high-Al and high-Ti, high-Cr and high-Ti).

The studied chromitites are high-Cr chromitites (Cr# > 60). High-Cr chromitites are related with high-Mg tholeitic or boninitic magma products (Irvine, 1977; Fisk, 1986; Kelemen et al., 1992; Arai, 1994; Zhou et al., 1996). Boninites are probably sulfur under-saturated Si-rich mafic magmas (Peck and Keays, 1990; Zhou et al., 1998). This type of magma may increase and support Cr spinel precipitation due to melt polymetalization formed by intense/widespread reaction with harzburgite (Peck and Keays, 1990; González-Jiménez et al., 2011). Experimental studies have shown that 20% partial melting of a fertile lherzolitic source produces a residual harzburgite (Bonatti and Michael, 1989; Kostopoulos, 1991). In the first stage of this melting a MORB-like melt composition is generated. Boninitic melts are derived from second stage melting of a refractory mantle and are enriched in volatiles derived from the subducting slab (Orberger et al., 1995; Pearce et al., 2000; Shervais, 2001; Page et al., 2008).

The geochemical composition of the chromite depends on its parental melt. Parental melt composition might be calculated using FeO/MgO and Al₂O₃ ratio in monomineralic chromite (Maurel and Maurel, 1982; Mondal et al., 2006; González-Jiménez et al., 2011). Parental melt compositions of the Group-I and Group-II chromitites were calculated by using FeO/MgO and Al₂O₃ ratios in the equations proposed by Maurel and Maurel (1982) { $(\text{Al}_2\text{O}_3)_{\text{spinel}} = 0.035 (\text{Al}_2\text{O}_3)_{\text{melt}}^{2.42}$ and $\text{Ln}(\text{FeO}/\text{MgO})_{\text{spinel}} = 0.47 - 1.07 \text{ Al}^{\#}_{\text{spinel}} + 0.64 \text{ Fe}^{3+} \# + \text{Ln}(\text{FeO}/\text{MgO})_{\text{melt}}$ }. Calculated parental melt compositions are 11.2–13.4 wt.% Al₂O₃ and 0.64–1.50 interval FeO/MgO ratio for Group-I chromitites, and 8.2–9.3 wt.% Al₂O₃ and 0.51–1.12 interval FeO/MgO ratio for Group-II chromitites. These results show that the parental melts of the examined chromitites are similar to boninite (MORB-like composition is 16 wt.% Al₂O₃ and 1.2–1.6 ratio of FeO/MgO ratio; boninitic composition is 10.6–14.4 wt.% Al₂O₃ and 0.7–1.4 ratio of FeO/MgO; from Wilson, 1989). Similar compositions are defined as high-Cr chromitites which have been reported in many areas (Table 5).

These similar parental melt compositions calculated from high-Cr chromitites support the idea that Group-I and Group-II chromitites crystallized from boninitic magma. Parental melt compositions of the examined chromitites fall in Thetford and Troodos boninitic field based on the TiO₂_{melt} versus Al₂O₃_{melt} diagram recommended by Page and Barnes (2009) (Fig. 6A).

Although both Group-I and Group-II chromitites have boninitic character, Group-II chromitites have higher Cr# and lower wt.% TiO₂ and Al₂O₃ content than Group-I. The differences in chromite, such as Cr rich and Al rich, have been identified in the same geodynamic environment (Leblanc and Nicolas, 1992; Zhou and Bai, 1992; Melcher et al., 1997; Kocks et al., 2007; Rollinson, 2008; Uysal et al., 2009b; Zaccarini et al., 2011; Dönmez et al., 2014). The relationship between bimodal distribution and vertical zonation of chromitites is known from different places (Rammlmair et al., 1987; Leblanc and Nicolas, 1992; Rollinson, 2008). While Cr-rich chromitites exist in deeper mantle, Al-rich chromitites can be found at stratigraphically higher levels. This situation can occur as a result of independent mechanisms. These mechanisms can develop in different ways, such as:

- i- Intrusions may be formed from different degrees of melting from depleted mantle sources,
- ii- Mixing of different magmas in SSZ areas,
- iii- Reactions between a parental melt (boninitic nature) and host-rocks characterized by different residual fractions,
- iv- Simultaneous fractional deposition after a high-Cr boninitic composition parental melt acquires a different character in the SSZ area (Zaccarini et al., 2011).

There is a general consensus that the parental melt character and stratigraphy of the mantle have significant effects on chromite chemistry for mantle-hosted chromitites (Rammlmair et al., 1987; Leblanc and Nicolas, 1992; Rollinson, 2008; González-Jiménez et al., 2011; Zaccarini et al., 2011). The mantle is in equilibrium with chromitites; geotectonic and stratigraphic affinity can be determined by using data from Kamenetsky et al. (2001), the approaches of Rollinson (2008) and the

Table 4
PGE concentrations (ppb) and calculated values for the Eastern Anatolia chromitites.

SAMPLE	Os	Ir	Ru	Rh	Pt	Pd	Σ PGE	Pd/Ir	IPGE/PPGE	Pt/Pt*
YBR-1	64	84	207	13	13	9	390	0.11	10.14	0.38
YBR-2	51	71	112	9	14	5	262	0.07	8.36	0.67
YBL-1	40	43	107	7	15	6	218	0.14	6.79	0.74
CE-1	19	27	59	7	10	5	127	0.19	4.77	0.54
ME-3	21	30	42	8	27	7	135	0.23	2.21	1.16
ME-4	18	42	95	13	24	10	202	0.24	3.30	0.67
MO-12	17	18	44	8	3	5	95	0.28	4.94	0.15
MO-26	12	19	31	8	4	5	79	0.26	3.65	0.20

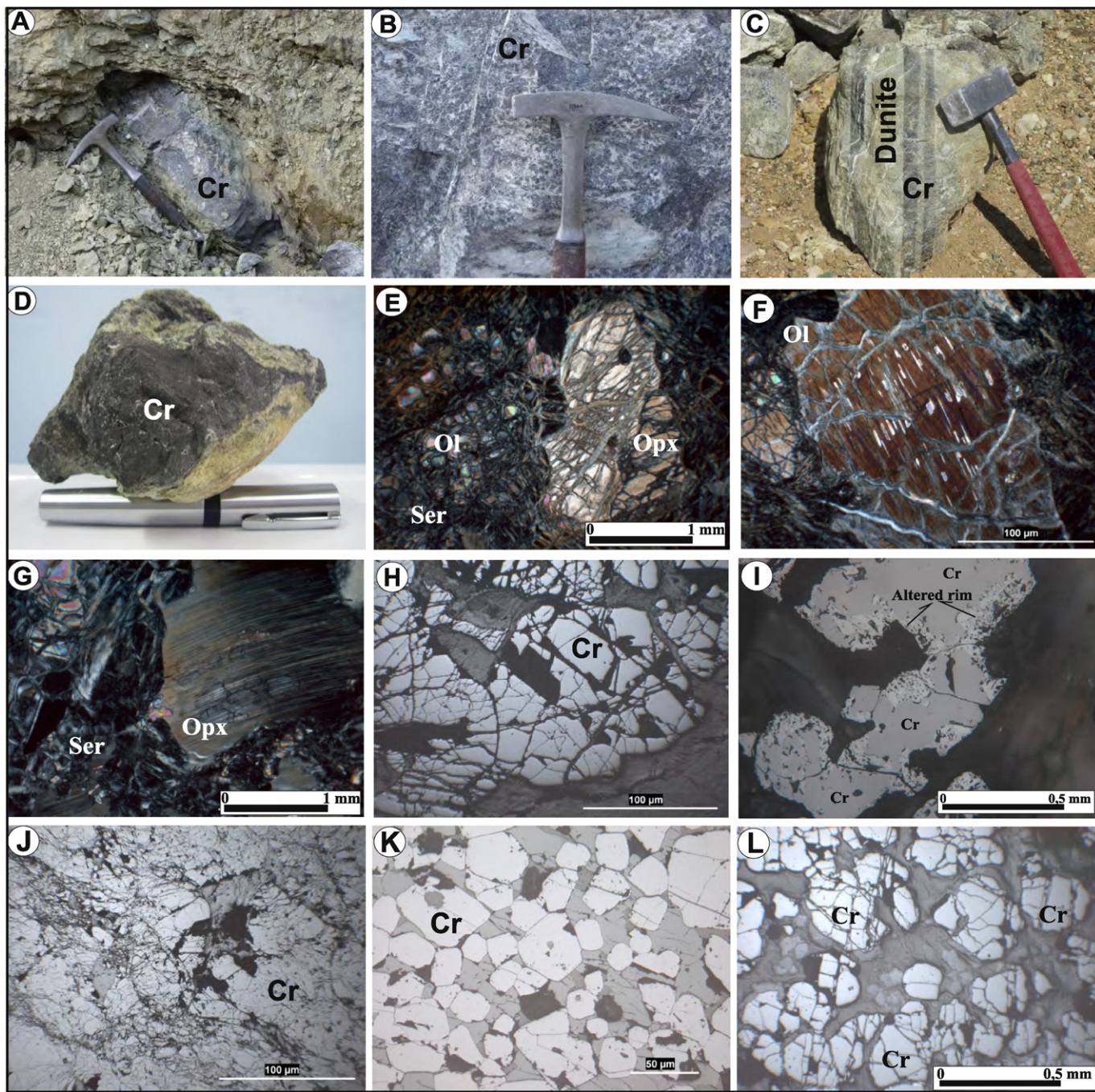


Fig. 2. Photographs and photomicrographs of chromitite and related harzburgite from the studied ophiolites: A) Massive chromitite, B) nodular chromitite, C) schlieren-banded chromitite, D) boudine shaped chromitite, E) porphyro-granoblastic and mesh texture of harzburgite, F-G) king band texture in orthopyroxene (harzburgite), H) chromite grains show high reflectivity, I) pale colored altered rim and crack of a chromite, J) cataclastic texture in massive chromitite, K) cumulate texture in schlieren-banded type chromitite, and L) pull-apart cracks in nodular chromitite (Ol—olivine, Opx—orthopyroxene, Ser—serpentine, Cr—chromite).

linear regression from Zaccarini et al. (2011). Group-I and Group-II chromitites show arc affinity on the Al_2O_3 melt versus Al_2O_3 diagram and Group-I chromitites show shallow emplacement affinity but Group-II chromitites fall in deeper environments (Fig. 6B), as seen in the Oman chromitite fields (Rollinson, 2008). Group-I and Group-II chromitites are distinctly separate on the Cr# versus to Cr/Fe diagram of Rammlmaier (1986). The fields numbered I and II are referred to as ultramafic tectonics locations and fields numbered III and IV refer to mafic-ultramafic cumulate (Fig. 6C). Region-I represents deep mantle chromitite fields and region-II represents shallow mantle chromitites that are underneath the MOHO (Fig. 6C). In this diagram, Group-II

chromitites are located in the deep mantle and Group-I chromitites are located in shallow mantle as is compatible with the melting model.

The Elazığ (Guleman chromitites/high-Cr) chromitites are economically important chromitite deposits in Turkey and were emplaced in the shallow mantle underneath the MOHO (Engin et al., 1981, 1986; Üşümezsoy, 1986; Çakır, 1994; Koptagel, 1996; Uçurum et al., 2006). Both Group-I chromitites and Elazığ (Guleman) chromitites are similar and they are interpreted to have been emplaced in shallow mantle based on the Cr# versus to Cr/Fe % diagram. These data indicate that shallow mantle emplacement chromitites are not only high-Al chromitites (Rollinson, 2008; González-Jiménez et al., 2011; Zaccarini

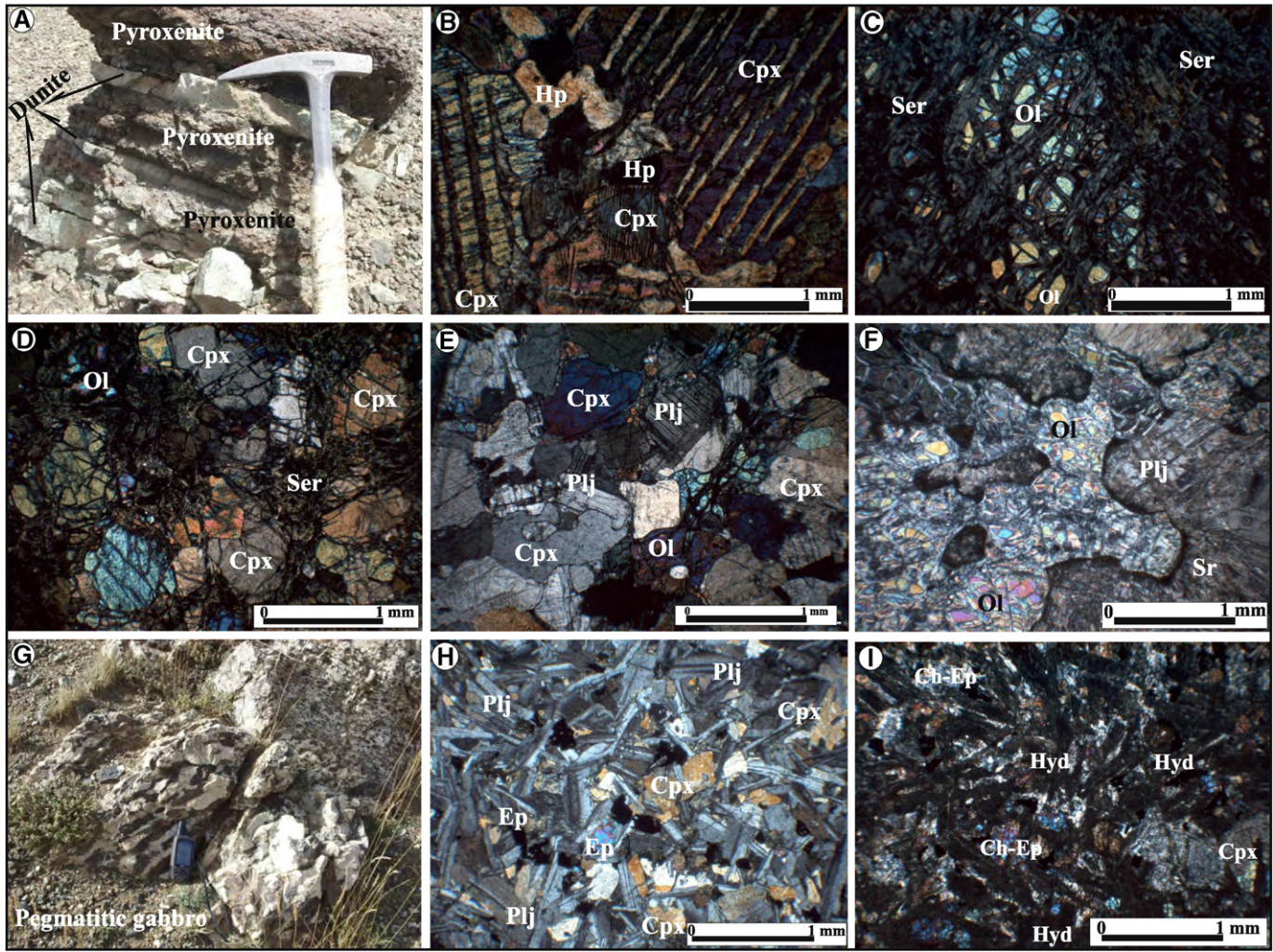


Fig. 3. Photographs and photomicrographs of different rock types from the studied ophiolites: A) Pyroxenite and dunite intercalation, B) pyroxenite (Cpx—clinopyroxene, Hp—hyperstene), C) dunite (Ol—olivine, Ser—serpentine), D) wherlite, E) olivine gabbro (Plj—plagioclase), F) troctolite (Sr—sericite), G) pegmatitic gabbro, H) diabase (Ep—epidote), and I) rodingitization of diabase (Hyd—hydrogrossular, Ch—chlorite).

et al., 2011; Dönmez et al., 2014) but high-Cr chromitites may also emplace in the shallow mantle.

Apart from the Elazığ chromitites, determining the stratigraphic location of Turkey's chromitites (Bursa-Eskişehir, Muğla, Sivas-Erzincan, Kastamonu-Çorum) in host rocks is difficult. This situation is due to the majority of ophiolites occurring in incomplete sequences and/or the lack of preservation of primary contact relationships of the ophiolite series. As chromitites are not found, yet, in certain stratigraphic levels of complete ophiolites or those where the full sequence is observed (especially Hatay-Kahramanmaraş), the relationship between the stratigraphic location and geochemical characteristics of chromitites cannot be fully explained. The location of the Elazığ (Guleman chromitites/high-Cr) chromitites within the ophiolitic unit is reported as i) massive chromitites surrounded by dunitic envelopes within harzburgite, ii) chromitites in harzburgite in the uppermost sections of tectonites below the cumulate sequences, iii) chromitites in dunites above tectonites just below the cumulate sequence (transition zone) and iv) chromitites in dunitic sections of the cumulate sequence (Engin et al., 1986). The geochemical characteristics of Elazığ chromitites determined by Uçurum et al. (2006) are similar to the Eastern Anatolia Ophiolite chromitites that are the topic of this paper. Additionally the Eastern Anatolia Ophiolites exhibit melange characteristics. There is no primary relationship with the sequence of the ophiolitic unit. As a result the stratigraphic location of the chromitites

cannot be determined in the ophiolitic unit in terms of time or space. However, markers of both the upper and lower levels of the mantle-crust transition zone of troctolite, olivine gabbro, gabbroic and diabasic dykes are found in close proximity to the investigated chromitites. This situation may be a weak indicator that the Eastern Anatolian chromitites had shallow mantle location.

7.2. The PGE concentration in chromitite

No relationship has been recognized between bulk rock PGE content and chromitite mineral chemistry in the examined chromitites. Generally there is a consensus that the ophiolitic chromitites have high IPGE/PPGE and low PGE values (Economou-Eliopoulos, 1996; Zhou et al., 1998; Proenza et al., 1998; Melcher et al., 1999; Ahmet and Arai, 2002; Garuti, 2004; Uysal et al., 2009a, 2009b; González-Jiménez et al., 2011; Zaccarini et al., 2011). Chondrite-normalized PGE patterns of the examined chromitites exhibit a negative trend from Ir to Pd group metals as seen in ophiolitic chromitites (Fig. 7A).

Geochemical behavior of the PGE petrologic process is implied as the Pd/Ir ratio is known as a differentiation index and the Pd/Ir ratio result of undifferentiated material should be 1 (Barnes et al., 1985; Garuti et al., 1997). The Pd and Ir ratio of the investigated chromitites varies from 0.07 to 0.28 and is consistent with rich an IPGE pattern. PGE data plotted on the total PGE vs PPGE_N/IPGE_N (Fig. 7B) diagram indicate the

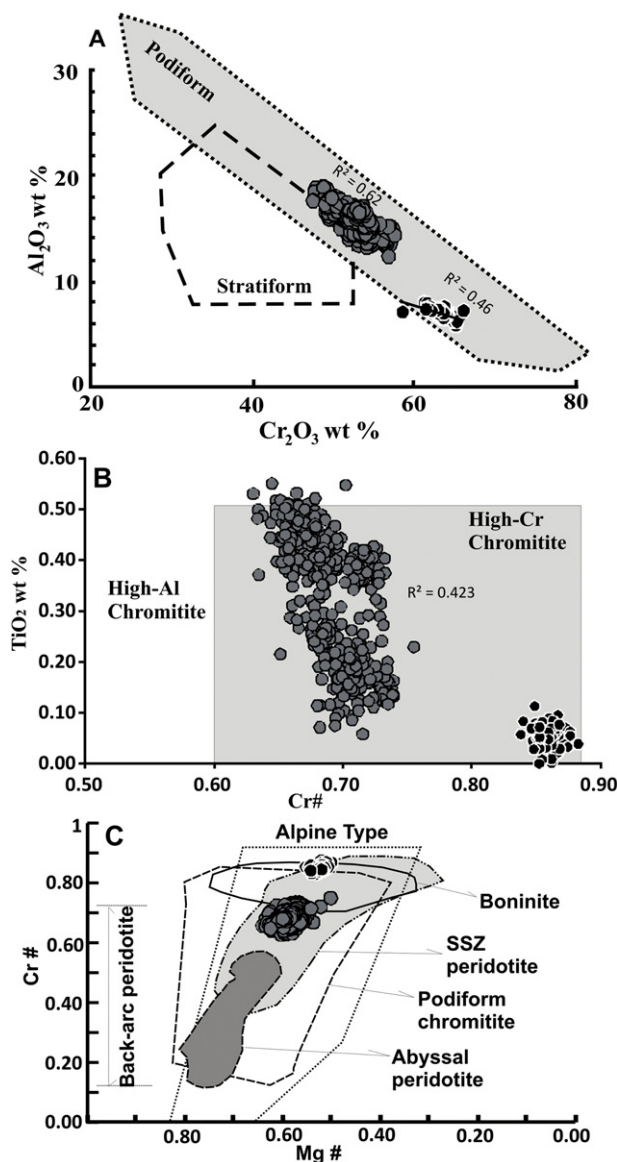


Fig. 4. Composition of chromite cores in chromite from four chromitite locations. A and B) negative correlation of Al_2O_3 versus Cr_2O_3 and TiO_2 versus $\text{Cr}\# = \text{Cr}/(\text{Cr} + \text{Al})$. C) Diagram of $\text{Cr}\#$ versus $\text{Mg}\# = \text{Mg}/(\text{Mg} + \text{Fe}^{+2})$. The podiform, stratiform fields and Alpine-type field are from Irvine (1967) and Leblanc and Nicolas (1992). The boninite field is from Ari (1992). The abyssal peridotite field is from Dick and Bullen (1984). Back-arc peridotite field is from Monnier et al. (1995). SSZ peridotite field is from Choi et al. (2008).

ophiolitic trend proposed by Melcher et al. (1999) and also total PGE has a negative trend with $\text{PPGE}_N/\text{IPGE}_N$. However, the data on Pd/Ir vs $\text{Pt}/\text{Pt}^* [= \text{Pt}_N/(\text{Rh}_N^*\text{Pd}_N)^{1/2}]$ diagrams (Garuti et al., 1997) show a partial melting trend rather than fractionation (Fig. 7C). These data show that parental melting created the examined chromitites, with Ir-group elements belonging to a primary phase of crystallization while Pd group elements stay in residual melts.

Boninites occurred from a depleted mantle source with a high degree re-melting ($>20\%$) and sulfur under saturated melting (Zhou et al., 1998). The sulfur under saturated melts determine the quantity of PGE that comes from these types of chromitites (Prichard et al., 1996). Crystallization of PGE-rich chromitites is in equilibrium with melts formulated in a critical melting interval between 20 and 25% (Prichard et al., 2008). Total PGE concentration is low in the examined chromitites (i.e. between 79 and 390 ppb). It probably indicates that the examined chromites come from parental melts that did not approach the necessary critical melting interval for enrichment of PGE.

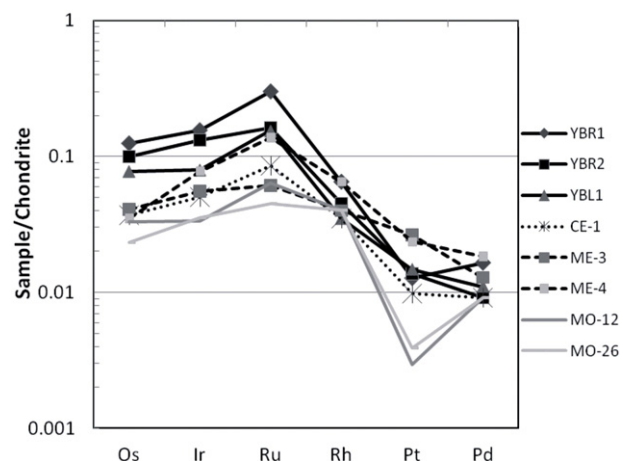


Fig. 5. Chondrite-normalized PGE patterns for podiform chromitite samples from the Van area ophiolite complex. Chondrite values from Naldrett and Duke (1980; cf. 514, 540, 690, 200, 1020 and 545 for Os, Ir, Ru, Rh, Pt and Pd, respectively).

In such a situation, while calcophile PPGE melt may remain, chromites precipitating from highly refractory and siderophile IPGE melt may enclose nano-sized crystals (Zaccarini et al., 2011). Experimental studies by Brenan and Andrews (2001) and Andrews and Brenan (2002) have revealed that partial melt, in addition to sulfur fugacity and temperature, plays an important role in the formation of Ir-group element alloys or sulfides. During chromite crystallization, formation of different Ir-group element minerals may be explained by “metal clustering” linked

Table 5
Comparison of parental melt compositions of this study at different area.

	High-Cr chromitites
Rollinson (2008) Oman ophiolite	$\text{Al}_2\text{O}_3\text{melt}: 11.8\text{--}12.9\text{ wt.\%}$ $\text{Cr}\#: 0.71\text{--}0.77$
Uysal et al. (2009b) Muğla ophiolite	$\text{Al}_2\text{O}_3\text{melt}: 8.8\text{--}10.5\text{ wt.\%}$ $\text{FeO}/\text{MgO}: 0.3\text{--}1.1$ $\text{Cr}\#: 0.64\text{--}0.85$
González-Jiménez et al. (2011) Sagua de Tanamo ophiolite	$\text{Al}_2\text{O}_3\text{melt}: 12.9\text{--}14.1\text{ wt.\%}$ $\text{FeO}/\text{MgO}: 0.9\text{--}1.5$ $\text{Cr}\#: 0.63\text{--}0.72$
Ghazi et al. (2011) Nain ophiolite	$\text{Al}_2\text{O}_3\text{melt}: 11.5\text{--}11.9\text{ wt.\%}$ $\text{FeO}/\text{MgO}: 0.83\text{--}0.84$ $\text{Cr}\#: 0.69\text{--}0.72$
Pal (2011) Andaman ophiolite	$\text{Al}_2\text{O}_3\text{melt}: 11.4\text{--}11.9\text{ wt.\%}$ $\text{FeO}/\text{MgO}: 0.56\text{--}0.69$ $\text{Cr}\#: 0.72\text{--}0.75$
Zaccarini et al. (2011) Santa Elena ophiolite	$\text{Al}_2\text{O}_3\text{melt}: 11.02\text{--}13.3\text{ wt.\%}$ $\text{Cr}\#: 0.61\text{--}0.80$
Dönmez et al. (2014) Elekdağ ophiolite	$\text{Al}_2\text{O}_3\text{melt}: 9.4\text{--}13.2\text{ wt.\%}$ $\text{FeO}/\text{MgO}: 0.4\text{--}1.9$ $\text{Cr}\#: 0.65\text{--}0.89$
<i>This study</i>	
Group-I chromitites	$\text{Al}_2\text{O}_3\text{melt}: 11.2\text{--}13.4\text{ wt.\%}$ $\text{FeO}/\text{MgO}: 0.64\text{--}1.50$ $\text{Cr}\#: 0.63\text{--}0.75$
Group-II chromitites	$\text{Al}_2\text{O}_3\text{melt}: 8.2\text{--}9.3\text{ wt.\%}$ $\text{FeO}/\text{MgO}: 0.51\text{--}1.12$ $\text{Cr}\#: 0.83\text{--}0.88$

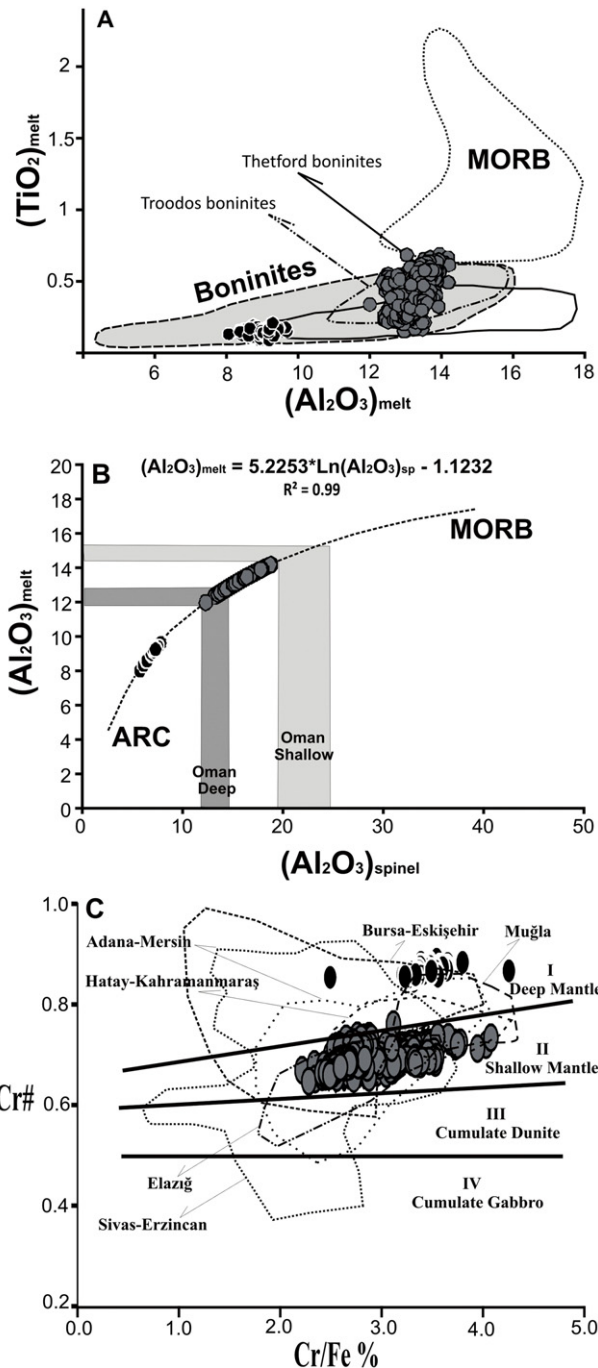


Fig. 6. A) TiO_2 and Al_2O_3 (wt.%) content of the melt calculated to be in equilibrium with chromite from the podiform chromitites in Eastern Turkey ophiolite. Boninates (Jenner, 1981; Walker and Cameron, 1983; Kamenetsky et al., 2002), Troodos boninates (Cameron, 1985; Flower and Levine, 1987), Thetford boninates (Page and Barnes, 2009), MORB (Shibata et al., 1979; Le Roex et al., 1987; Presnall and Hoover, 1987). B) Calculated Al_2O_3 contents in parental melts of chromitite from the Van area ophiolites. Regression lines for MORB and ARC lavas are based on Kamenetsky et al. (2001); Rollinson (2008) and Zaccarini et al. (2011). C) $\text{Cr}^{\#}$ versus Cr/Fe (wt.%) diagram (Rammlair, 1986), Turkish ophiolitic chromitite range on diagram (Uçurum et al., 2006).

to appropriate sulfur fugacity and temperature conditions of the parental melt (Tredoux et al., 1995).

7.3. Significance and tectonic setting of the chromitites

Chrome spinel chemistry variety is related with high petrologic heterogeneity of mantle section (Lippard et al., 1986) which can develop

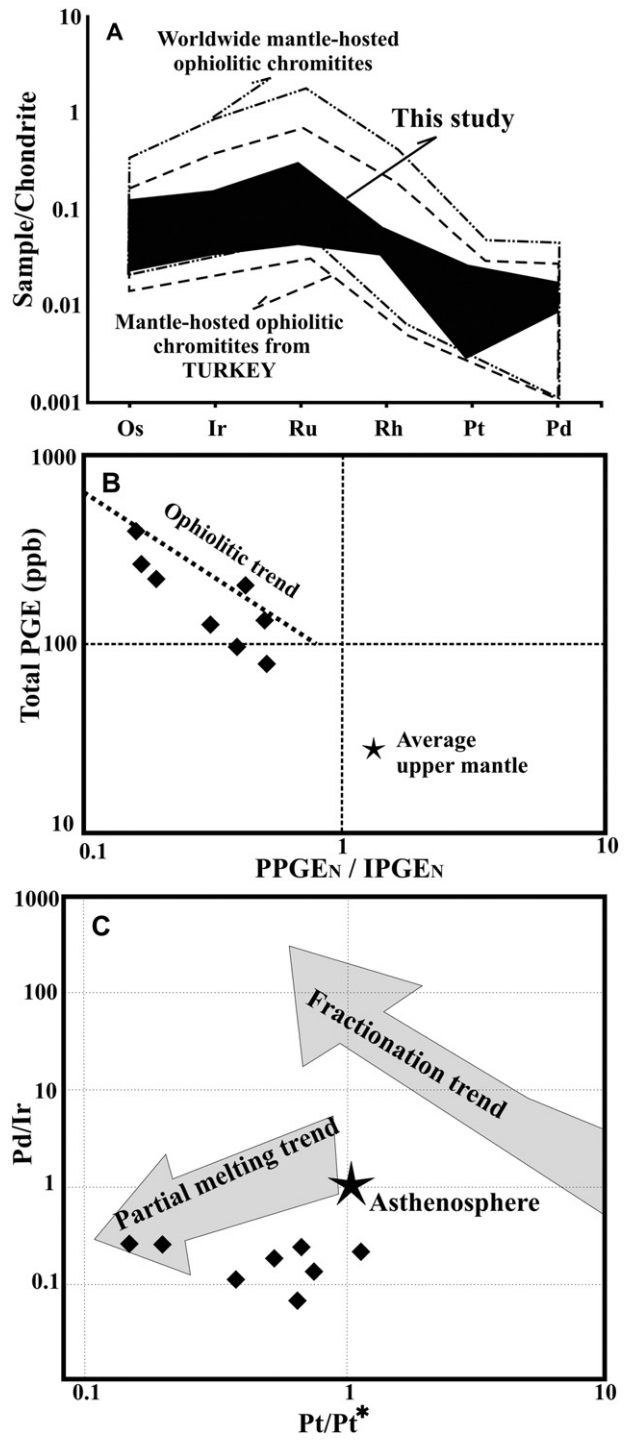


Fig. 7. A – Chondrite-normalized PGE patterns for investigated chromitites, chondrite normalization values from Naldrett and Duke (1980), field of mantle-hosted ophiolitic chromitite of worldwide (after McElduff and Stumpf, 1990; Economou-Eliopoulos, 1996; Melcher et al., 1997; Proenza et al., 1999; Garuti et al., 2005), field of mantle-hosted ophiolitic chromitites from the Turkey (after Page et al., 1984; Yaman and Ohnenstetter, 1991; Başpınar, 2006; Uçurum et al., 2006; Uysal et al., 2007a, 2007b; Uysal et al., 2009a, 2009b; Akbulut et al., 2010; Günay and Çolakoğlu, 2011; Dönmez et al., 2014). B – total PGE vs PPGEN/IPGEN diagram (Melcher et al., 1999). C – Pd/Ir vs Pt/Pt^* [$= \text{PtN}/(\text{Rh}^*\text{PdN})^{1/2}$] diagram (Garuti et al., 1997).

as a result of peridotite magma reactions (Arai et al., 2006, 2011). Chrome spinel chemistry variety of mantle hosted chromitites may be due to:

- During the evolution of oceanic crust, ophiolite environments are from different sources for different durations (Melcher et al.,

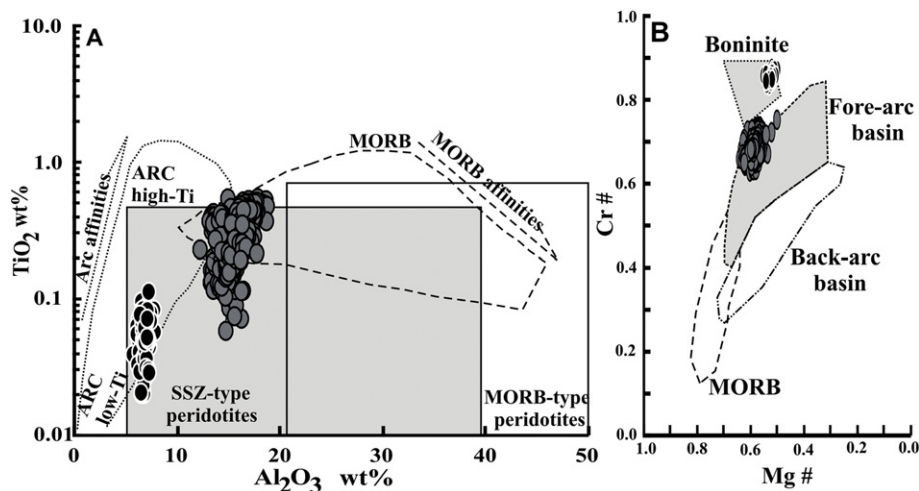


Fig. 8. A – Al_2O_3 – TiO_2 relationship of examined chromitites (Kamenetsky et al., 2001), B – Cr-number vs. Mg-number diagram of Dick and Bullen (1984).

- 1997; Zhou and Robinson, 1997; Zhou et al., 1998; Uysal et al., 2009b),
- ii) Initially, progressive fraction of Cr-rich melting at fore-arc (Graham et al., 1996),
 - iii) Under the MOHO transition zone shallower and deeper processes (Rollinson, 2008)
 - iv) It can be related to different melting of intrusions occurring in different mantle sources, in a back arc basin setting, with temporal and/or spatial differences (González-Jiménez et al., 2011)

Chrome spinel chemistry can be used to estimate the origin of parental magma and tectonic setting of host-rocks (Dick and Bullen, 1984; Kamenetsky et al., 2001; Arai et al., 2011). As a general consensus high Cr# (>0.6) and low TiO_2 wt.% (<0.3) component of chromite spinels possibly conform to arc rocks (Arai et al., 2006), oceanic crust rocks (MORB and ultramafic rocks) have lower Cr# (>0.60) than arc spinels (Dick and Bullen, 1984; Zhou et al., 1994; Niu and Heikinian, 1997; Kamenetsky et al., 2001; Arai et al., 2006, 2011).

The relationship between TiO_2 wt.% and Al_2O_3 wt.% in chrome spinels shows a negative correlation for MORB-type chrome spinels and positive correlation for arc-type chrome spinels (Kamenetsky et al., 2001; Rollinson, 2008; Zaccarini et al., 2011). High Cr# (63–88), Mg# (50–64) values and low TiO_2 (0.01–0.5 wt.%) and Al_2O_3 (5.7–18.8 wt.%) component of Eastern Anatolia ophiolitic chromites indicate that they are related to a supra subduction zone tectonic environment (Fig. 8A). The parental melt composition for the examined chromitites is boninitic composition, which indicates a reaction between boninitic melts for chromitite occurrence and refractory peridotites. These types of melt–rock interaction trends and the relationship with TiO_2 versus Al_2O_3 and Cr# versus Mg# of chrome spinels suggest there was a fore-arc tectonomagmatic environment for Eastern Anatolia ophiolitic chromitites (Parkinson and Pearce, 1998; Okamura et al., 2006; Fig. 8B).

The ophiolitic units in the Eastern Anatolia are situated along an E–W trend. Ophiolite units without volcanic sequences have not only mélange character sections but also huge mantle peridotite slabs. The petrogenesis and geochronological age data belonging to isolated diabase dikes cutting the peridotites among the examined chromitites indicate that existing intra-oceanic subduction developed in the Late Cretaceous at the time of closure of the south branch of the Neotethyan ocean (Günay, 2011; Çolakoğlu et al., 2012; Günay et al., 2012). These diabase dikes exhibit supra subduction zone (SSZ), enriched MORB (E-MORB) and oceanic-island basalt (OIB) type geochemical features. Based on close geochronological ages, it is interpreted that these diabase dikes with three different geochemical characteristics formed in the same SSZ tectonomagmatic environment (Çolakoğlu et al., 2012). Isolated diabase dikes may have formed not just from enriched magma but

from depleted magma caused by slab roll-back leading to decompression melting (Çolakoğlu et al., 2012).

The Alabayır chromitites, located in Group-I as proposed by Çolakoğlu et al. (2012), are cut by OIB type diabase dikes. It may indicate that the Group-1 chromitites (Alabayır chromitites) formed in a fore-arc tectonomagmatic environment cut by OIB type diabase that may have formed in the SSZ geotectonic environment. This increases the likelihood of the slab roll back mechanism as proposed by Çolakoğlu et al. (2012), may have existed.

8. Conclusions

This paper presents the first detailed investigation of mantle chromitites in Eastern Turkey located at Alabayır, Mehmetalan, Mollatopuz and Yukarıbalçaklı areas of the Van region.

The studied chromitites were divided into two groups and their mineral chemistry indicates that they are high-Cr chromitites. Calculated parental melt composition of Group-I (Alabayır, Mollatopuz, Yukarıbalçaklı and Mehmetalan-I chromitites) and Group-II (Mehmetalan-II chromitites) chromitites show that they formed from boninitic magma. Mineral chemistry and parental melt compositions of the studied chromitites have shown that they formed in different environments. While Group-II chromitites formed in deeper parts of the mantle environment, whereas Group-I chromitites formed in shallow parts of the mantle at or near the MOHO transition zone. Based on the PGE geochemistry and chromite compositions, PGE abundance is characteristic of the IPGE group and similar to podiform chromitite in ophiolitic terranes. The chromitite occurrences were formed in a fore-arc tectonomagmatic environment from a parental magma with boninitic character and were cut by OIB type diabase dikes, therefore most probably a slab roll-back mechanism can be considered for the Neotethys Ocean in this region.

Acknowledgments

This research has been supported by TUBİTAK (Project No: CAYDAG-108Y209). The authors appreciate the useful comments and suggestions made by Franco Pirajno, Osman Parlak, David Bickford, Ibrahim Uysal and the manuscript reviewers. The authors wish to thank Cahit Dönmez and Catherine Yiğit for their support in the writing of the manuscript.

Appendix A. Supplementary data

Supplementary data associated with this article can be found in the online version, at <http://dx.doi.org/10.1016/j.oregeorev.2015.10.021>. These data include the Google map of the most important areas described in this article.

References

- Acarlar, M., Bilgin, A., Erkal, T., Güner, E., Sen, A., Umut, M., Elbilo, E., Gedik, İ., Hakyemez, Y., Uguz, F., 1991. Geology of northern and eastern part of Lake Van. General Directorate of Mineral Research and Exploration, Turkey Open File Report Nr. 9469. 94 pp. (unpublished).
- Ahmet, A.H., Arai, S., 2002. Unexpectedly high-PGE chromitite from the deeper mantle section of the northern Oman ophiolite and its tectonic implications. *Contrib. Mineral. Petro.* 143, 263–278.
- Akulut, M., Pişkin, Ö., Arai, S., Özgenç, I., Minareci, F., 2010. Base metal (BM) and platinum-group elements (PGE) mineralogy and geochemistry of the Elmaslar chromite deposit (Denizli, SW Turkey): implications for a local BM and PGE enrichment. *Ophioliti* 35 (1), 1–20.
- Andrews, D.R.A., Brenan, J.M., 2002. Phase equilibrium constraints on the magmatic origin of laurite + Ru-Os-Ir alloy. *Can. Mineral.* 40, 1705–1716.
- Arai, S., 1992. Chemistry of chromian spinel in volcanic rocks as a potential guide to magma chemistry mineral. *Mag.* 56, 173–184.
- Arai, S., 1994. Compositional variation of olivine chromian spinel in Mg-rich magmas as a guide to their residual spinel peridotites. *J. Volcanol. Geotherm. Res.* 59, 279–294.
- Arai, S., 1997. Origin of podiform chromitites. *J. Asian Earth Sci.* 15, 303–310.
- Arai, S., Kadoshima, K., Morishita, T., 2006. Widespread arc-related melting in the mantle section of the northern Oman ophiolite as inferred from detrital chromian spinels. *J. Geol. Soc. Lond.* 163, 869–879.
- Arai, S., Okamura, H., Kadoshima, K., Tanaka, C., Suzuki, K., Ishimaru, S., 2011. Chemical characteristics of chromian spinel in plutonic rocks: implications for deep magma processes and discrimination of tectonic setting. *Island Arc* 20, 125–137.
- Arai, S., Uesugi, J., Ahmed, A.H., 2004. Upper crustal podiform chromitite from the northern Oman ophiolite as the stratigraphically shallowest chromitite in ophiolite and its implication for Cr concentration. *Contrib. Mineral. Petro.* 147, 145–154.
- Ballhaus, C., 1998. Origin of podiform chromite deposits by magma mingling. *Earth Planet. Sci. Lett.* 156, 185–193.
- Barnes, S.J., Naldrett, A.J., Gorton, M.P., 1985. The origin of platinum group elements in terrestrial magmas. *Chem. Geol.* 53, 303–323.
- Başpinar, G., 2006. Guleman (Elazığ) Bölgesi Krom Yataklarının Platin Grubu Element İçerikleri ve Jeokimyası (Master thesis) Fırat University, Institute of Science and Technology, 138 p (unpublished), Elazığ.
- Bonatti, E., Michael, P.J., 1989. Mantle peridotites from continental rifts to ocean basins to subduction zones. *Earth Planet. Sci. Lett.* 91, 297–311.
- Brenan, J.M., Andrews, D.R.A., 2001. High-temperature stability of laurite and Ru-Os-Ir alloys and their role in PGE fractionation in mafic magmas. *Can. Mineral.* 39, 341–360.
- Çakır, Ü., 1994. Batı Kef krom yatağınnın (Guleman-Elazığ) Jeolojik Özellikleri. *Türk. Jeol. Bül.* 37 (2), 15–29.
- Cameron, W.E., 1985. Petrology and origin of primitive lavas from the Troodos ophiolite Cyprus. *Contrib. Mineral. Petro.* 89, 239–255.
- Choi, S.H., Shervais, J.W., Mukasa, S.B., 2008. Supra-subduction and abyssal mantle peridotites of the Coast Range ophiolite, California. *Contrib. Mineral. Petro.* 156, 551–576.
- Çolakoglu, A.R., Arehart, B.G., 2010. The petrogenesis of Sarıçimen (Caldiran-Van) quartz monzonodiorite: implication for initiation of magmatism (Late Middle Miocene) in the East Anatolian collision zone, Turkey. *Lithos* 119, 607–620.
- Çolakoglu, A.R., Sayit, K., Günay, K., Göncüoğlu, M.C., 2012. Geochemistry of mafic dykes from the Southeast Anatolian ophiolites, Turkey: Implications for an intra-oceanic arc-basin system. *Lithos* 132–133, 113–126.
- Çolakoglu, A.R., Günay, K., Göncüoğlu, M.C., Oyan, V., Erdoğan, K., 2014. Geochemical evaluation of the late maastrichtian subduction-related volcanism in the southern neotethys in Van area, and a correlation across the Turkish–Iranian border. *Ophioliti* 39 (2), 51–65 2014.
- Dewey, J.F., Hempton, M.R., Kidd, W.S.F., Şaroğlu, F., Şengör, A.M.C., 1986. Shortening of continental lithosphere: the neotectonics of Eastern Anatolia – a young collision zone. In: Coward, M.P., Ries, A.C. (Eds.), Collision Tectonics. Geological Society special publication 19, pp. 3–36 (1986).
- Dick, H.J.B., Bullen, T., 1984. Chromian spinel as a petrogenetic indicator in abyssal and Alpine-type peridotites and spatially associated lavas. *Contrib. Mineral. Petro.* 86, 54–76.
- Dickey, J.S., 1975. A hypothesis of origin for podiform chromite deposits. *Geochim. Cosmochim. Acta* 39, 1061–1074.
- Dönmez, C., Keskin, S., Günay, K., Çolakoglu, A.O., Çiftçi, Y., Uysal, İ., Türkel, A., Yıldırım, N., 2014. Chromite and PGE geochemistry of the Elekdağ ophiolite (Kastamonu–northern Turkey): implications for deep magmatic processes in a supra-subduction zone setting. *Ore Geol. Rev.* 57, 216–228.
- Economou-Eliopoulos, M., 1996. Platinum-group elements distribution in chromite ores from ophiolite complexes: implications for their exploration. *Ore Geol. Rev.* 11, 363–381.
- Engin, T., Balci, M., Sümer, Y., Özkan, Y.Z., 1981. Guleman (Elazığ) kromyatakları ve Peridotit Birimi'nin genel jeoloji konumu ve yapısal özelliklerini. *Bull. Mineral. Res. Explor. Inst. Turk.* 95–96, 77–100.
- Engin, T., Ozkocak, O., Artan, U., 1986. General Geological Setting and Character of Chromite Deposits in Turkey, in Chromites, UNESCO's IGCP-197 Project Metallogeny of Ophiolites. Athens. Theopastus Publishers, Greece, pp. 199–228.
- Fisk, M.R., 1986. Basalt magma interaction with harzburgite and the formation of highmagnesian andesites. *Geophys. Res. Lett.* 13, 467–470.
- Flower, M.F.J., Levine, H.M., 1987. Petrogenesis of a tholeiite–boninite sequence from Ayios Mamas, Troodos ophiolite: evidence for splitting of a volcanic arc? *Contrib. Mineral. Petro.* 97, 509–524.
- Garuti, G., 2004. Chromite–platinum group element magmatic deposits. In: De Vivo, B., Stüwe, K. (Eds.), Geology, Encyclopedia of Life Support Systems (EOLSS). UNESCO, EOLSS Publisher, Oxford (United Kingdom) (<http://www.eolss.net>).
- Garuti, G., Fershtater, G., Bea, F., Montero, P.G., Pushkarev, E.V., Zaccarini, F., 1997. Platinum-group element distribution in mafic–ultramafic complexes of central and southern Urals: preliminary results. *Tectonophysics* 276, 181–194.
- Garuti, G., Proenza, J.A., Zaccarini, F., 2007. Distribution and mineralogy of platinum-group elements in altered chromitites of the Campo Formoso layered intrusion (Bahia State, Brazil): control by magmatic and hydrothermal processes. *Mineral. Petrol.* 89, 159–188.
- Garuti, G., Pushkarev, E.V., Zaccarini, F., 2005. Diversity of chromite–PGE mineralization in ultramafic complexes of the Urals. In: Törmänen, T.O., Alapieti, T.T. (Eds.), Platinum Group Elements – From Genesis to Beneficiation and Environmental Impact. Oulu (Finland), August 8–11, 10th International Platinum Symposium, Extended Abstracts, pp. 341–344.
- Ghazi, J.M., Moazzen, M., Rahghoshay, M., Moghadam, H.S., 2011. The geodynamic setting of the Nain ophiolites, Central Iran: evidence from chromian spinels in the chromitites and associated rocks. *Ophioliti* 36 (1), 59–76.
- Göncüoğlu, M.C., Dirik, K., Koçlu, H., 1997. Pre-Alpine and Alpine terranes in Turkey: explanatory notes to the terrane map of Turkey. *Ann. Géol. Pays Hellén.* 37, 515–536.
- González-Jiménez, J.M., Kerestedjian, T., Proenza, J.A., Gervilla, F., 2009. Metamorphism on chromite ores from the Dobromirtsi ultramafic massif, Rhodope Mountains (SE Bulgaria). *Geol. Acta* 7 (4), 413–429.
- González-Jiménez, J.M., Proenza, J.A., Gervilla, F., Melgarejo, J.C., Blanco-Moreno, J.A., Ruiz-Sánchez, R., Griffin, W.L., 2011. High-Cr and high-Al chromitites from the Sagua de Táamo district, Mayarí–Cristal ophiolitic massif (eastern Cuba): constraints on their origin from mineralogy and geochemistry of chromian spinel and platinum group elements. *Lithos* 125, 101–121.
- Graham, I.T., Franklin, B.J., Marshall, B., 1996. Chemistry and mineralogy of podiform chromitite deposits, southern NSW, Australia: a guide to their origin and evolution. *Mineral. Petrol.* 37, 129–150.
- Günay, K., 2011. Van-Özalp Çevresindeki Ophiolitlerin Jeolojisi, Petrolojisi ve Krom Cevherlemeleri (Phd Thesis), Yüzüncü Yıl University, Institute of Science and Technology, 274 pp (unpublished) Van.
- Günay, K., Çolakoglu, A.Ç., 2011. Geochemical properties and platinum group element (PGE) contents of eastern Turkey (Van area) chromitite. *Geol. Bull. Turk.* 54 (1–2), 1–24.
- Günay, K., Çolakoglu, A.R., Çakır, Ü., 2012. Geochemical properties and rodingitization of diabase dykes cutting peridotites in Yüksekova complex (Özalp, Van – Turkey). *Bull. Mineral. Res. Explor. Inst. Turk.* 144, 1–22.
- Innocenti, F., Mazzuoli, R., Pasquare, G., Radicati di Brozolo, F., Villari, L., 1976. Evolution of the volcanism in the area of interaction between the Arabian, Anatolian and Iranian plates (Lake Van, Eastern Turkey). *J. Volcanol. Geotherm. Res.* 1, 103–112.
- Irvine, T.N., 1967. Chromium spinels as a petrogenetic indicator petrologic applications. *Can. J. Earth Sci.* 11 (4), 71–103.
- Irvine, T.N., 1977. Origin of chromite layers in the Muskox intrusion and other intrusions: a new interpretation. *Geology* 5, 273–277.
- Jenner, G.A., 1981. Geochemistry of high-Mg andesites from Cape Vogel, Papua New Guinea. *Chem. Geol.* 33, 307–332.
- Kamenetsky, V.S., Crawford, A.J., Meffre, S., 2001. Factors controlling chemistry of magmatic spinel: an empirical study of associated olivine, Cr-spinel and melt inclusions from primitive rocks. *J. Petrol.* 42, 655–671.
- Kamenetsky, V.S., Sobolev, A.V., Eggins, S.M., Crawford, A.J., Arculus, R.J., 2002. Olivine-enriched melt inclusions in chromites from low-Ca boninites, Cape Vogel, Papua New Guinea: evidence for ultramafic primary magma, refractory mantle source and enriched components. *Chem. Geol.* 183, 287–303.
- Karaoglan, F., Parlak, O., Klötzli, U., Köller, F., Rizooglu, T., 2013. Age and duration of intra-oceanic arc volcanism built on a supra-subduction zone type oceanic crust in Southern Neotethys SE Anatolia. *Geosci. Front.* 4, 399–408.
- Karaoglan, F., Parlak, O., Klötzli, U., Thöni, M., Köller, F., 2014. U–Pb and Sm–Nd geochronology of the ophiolites from the SE Turkey: implication for the Neotethyan evolution. *Geodin. Acta* 25, 146–161.
- Kelemen, P.B., Dick, H.J.B., Quick, J.E., 1992. Formation of harzburgite by pervasive melt/rock interaction in the upper mantle. *Nature* 358, 635–641.
- Keskin, M., 2005. Domal uplift and volcanism in a collision zone without a mantle plume: evidence from Eastern Anatolia. www.MantlePlumes.org (38 pp.).
- Ketin, İ., 1983. Türkiye Jeolojisine Genel Bakış. ITÜ Kütüphanesi 1259 (595 pp.).
- Kocks, H., Melcher, F., Meisel, T., Burgath, K.P., 2007. Diverse contributing sources to chromite petrogenesis in the Shebenik ophiolitic complex, Albania: evidence from new PGE- and Os-isotope data. *Mineral. Petrol.* 91, 139–170.
- Koptagel, O., 1996. Türkiye'deki Bazı Kromitlerin Ana Bileşen Kimyası Özellikleri. Cumhuriyet Üniversitesi, Jeoloji Mühendisliği Dergisi 48, 22–26.
- Kostopoulos, D.K., 1991. Melting of shallow upper mantle: a new perspective. *J. Petrol.* 32, 671–699.
- Koçlu, H., Prichard, H., Melcher, F., Fisher, C.P., Brough, P.C., Stueben, D., 2014. Platinum group element (PGE) mineralisation and chromite geochemistry in the Berit ophiolite (Elbistan/Kahramanmaraş), SE Turkey. *Ore Geol. Rev.* 60, 97–111.
- Lago, B.L., Rabinow, C.Z.M., Nicolas, A., 1982. Podiform chromite ore bodies: a genetic model. *J. Petrol.* 23, 103–125.
- Le Roex, A.P., Dick, H.J.B., Gulen, L., Reid, A.M., Erlank, A.J., 1987. Local and regional heterogeneity in MORB from the mid-Atlantic ridge between 54.5°S and 51°S: evidence for geochemical enrichment. *Geochim. Cosmochim. Acta* 51, 541–555.
- Leblanc, M., Nicolas, A., 1992. Ophiolitic chromitites. *Int. Geol. Rev.* 34, 653–686.
- Lippard, S.J., Shelton, A.W., Gass, I.G., 1986. The ophiolite of Northern Oman. Geological Society Memoir No. 11. Geological Society, London.
- Maurel, C., Maurel, P., 1982. Étude expérimentale de la distribution de l'aluminium entre bain silicaté basique et spinelle chromifère. Implications pétrogénétiques: teneur en chrome des spinelles. *Bull. Mineral.* 105, 197–202.
- McElduff, B., Stumpf, E.F., 1990. The chromite deposits of the Troodos complex, Cyprus – evidence for the role of a fluid phase accompanying chromite formation. *Mineral. Deposita* 26, 307–318.

- Melcher, F., Grum, W., Simon, G., Thalhammer, T.V., Stumpf, F.E., 1997. Petrogenesis of the ophiolitic giant chromite deposits of Kempirsai, Kazakhstan: a study of solid and fluid inclusions in chromite. *J. Petrol.* 38, 1419–1438.
- Melcher, F., Grum, W., Thalhammer, T.V., Thalhammer, O.A.R., 1999. The giant chromite deposits at Kempirsai, Urals: constraints from trace element (PGE, REE) and isotope data. *Mineral. Deposita* 34, 250–272.
- Mondal, S.K., Ripley, E.M., Li, C., Frei, R., 2006. The genesis of Archaean chromitites from the Nuasah and Sukinda massifs in the Singhbhum Craton, India. *Precambrian Res.* 148, 45–66.
- Monnier, C., Girardeau, J., Maury, R., Cotten, J., 1995. Back-arc basin origin for the East Sulawesi ophiolite (eastern Indonesia). *Geology* 23, 851–854.
- Naldrett, A.J., Duke, J.M., 1980. Platinum metals in magmatic sulfide ores. *Science* 208, 1417–1424.
- Niu, Y., Heikinian, R., 1997. Spreading-rate dependence of the extent of mantle melting beneath ocean ridges. *Nature* 385, 326–329.
- Oberhaensli, R., Candan, O., Çetinkaplan, M., Koralay, E., Bousquet, R., 2012. The East Anatolian High-Temperature Belt. Proceed. 65th Geol. Congress, p. 87 (Abstract, Vol.).
- Okamura, H., Arai, S., Kim, Y.U., 2006. Petrology of forearc peridotite from the Hahajima Seamount, the Izu-Bonin arc, with special reference to chemical characteristics of chromian spinel. *Mineral. Mag.* 70, 15–26.
- Okay, A.I., Tüysüz, O., 1999. Tethyan sutures of northern Turkey. In: Durand, B., Jolivet, L., Horvath, F., Seranne, M. (Eds.), *The Mediterranean Basins: Tertiary Extinction Within the Alpine Orogen*. Geological Society, London, Special Publications 156, pp. 475–515.
- Okay, N., Zack, T., Okay, A.I., Barth, M., 2010. Sinistral transport along the Trans-European Suture Zone: detrital zircon-rutile geochronology and sandstone petrography from the carboniferous flysch of the Pontides. *Geol. Mag.* 148, 380–403.
- Orberger, B., Lorandb, J.P., Girardeau, J., Merciera, J.C.C., Pitragool, S., 1995. Petrogenesis of ultramafic rocks and associated chromitites in the Nan Uttaratid ophiolite, northern Thailand. *Lithos* 35, 153–182.
- Page, N.J., Engin, T., Singer, D.A., Haftty, J., 1984. Distribution of platinum-group elements in the Bati Kef chromite deposit, Güleman-Elazığ area, eastern Turkey. *Econ. Geol.* 79, 177–184.
- Page, P., Barnes, S.J., 2009. Using trace elements in chromites to constrain the origin of podiform chromitites in the Thetford Mines Ophiolite, Québec, Canada. *Econ. Geol.* 104, 997–1018.
- Page, P., Bédard, J.H., Schroetter, J.-M., Tremblay, A., 2008. Mantle petrology and mineralogy of the Thetford Mines Ophiolite Complex. *Lithos* 100, 255–292.
- Paktunc, A.D., 1990. Origin of the podiform chromite deposits by multistage melting, melt segregation and magma mixing in the upper mantle. *Ore Geol. Rev.* 5, 211–222.
- Pal, T., 2011. Petrology and geochemistry of the Andaman ophiolite: melt-rock interaction in a suprasubduction-zone setting. *J. Geol. Soc. Lond.* 168, 1031–1045.
- Parkinson, I.J., Pearce, J.A., 1998. Peridotites from the Izu–Bonin–Mariana forearc (ODP Leg 125): evidence for mantle melting and melt–mantle interaction in a suprasubduction zone setting. *J. Petrol.* 39, 1577–1618.
- Parlak, O., Çolakoğlu, A., Dönmez, C., Sayak, H., Yıldırım, N., Türköl, A., Odabaşı, İ., 2012. Geochemistry and Tectonic Significance of Ophiolites Along the Ankara-Erzincan Suture Zone in Northeastern Anatolia. In: Robertson, A.H.F., Parlak, O., Ünlügenç, U.C. (Eds.), *Geological Society, London, Special Publication* 372, pp. 75–106.
- Pearce, J.A., Barker, P.F., Edwards, S.J., Parkinson, I.J., Leat, P.T., 2000. Geochemistry and tectonic significance of peridotites from the South Sandwich arc–basin system, South Atlantic. *Contrib. Mineral. Petrol.* 139, 36–53.
- Peck, D.C., Keays, R.R., 1990. Geology, geochemistry, and origin of platinum-group element-chromitite occurrences in the Hazlewood River Complex, Tasmania. *Econ. Geol.* 85, 765–793.
- Presnall, D.C., Hoover, J.D., 1987. High pressure phase equilibrium constraints on the origin of mid-ocean ridge basalts. *Geochem. Soc. Spec. Pap.* 1, 75–89.
- Prichard, H.M., Lord, R.A., 1990. Platinum and palladium in the Troodos ophiolite complex, Cyprus. *Can. Mineral.* 28 (3), 607–617.
- Prichard, H.M., Lord, R.A., Neary, C.R., 1996. A model to explain the occurrence of platinum- and palladium-rich ophiolite complexes. *J. Geol. Soc.* 153, 323–328.
- Prichard, H.M., Neary, C.R., Fisher, P.C., O'Hara, M.J., 2008. PGE-rich podiform chromitites in the Al'Ays ophiolite complex, Saudi Arabia: an example of critical mantle melting to extract and concentrate PGE. *Econ. Geol.* 103 (7), 1507–1529.
- Proenza, J.A., Gervilla, F., Melgarejo, J.C., Bodinier, J.L., 1999. Al and Cr rich chromitites from the Mayarí–Baracoa Ophiolitic Belt (eastern Cuba): consequence of interaction between volatile-rich melts and peridotite in suprasubduction mantle. *Econ. Geol.* 94, 547–566.
- Proenza, J.A., Gervilla, F., Melgarejo, J.C., Reve, D., Rodríguez, Y.G., 1998. Ophiolitic chromitites from the Mercedita deposit (Cuba). Example of Al-rich chromites at the mantle–crust transition zone. *Acta Geol. Hisp.* 33, 179–212.
- Proenza, J.A., Ortega-Gutiérrez, F., Camprubí, A., Tritlla, J., Elías-Herrera, M., Reyes-Salas, M., 2004. Paleozoic serpentinite enclosed chromitites from Tehuitzingo, (Acatlán Complex, southern Mexico): a petrological and mineralogical study. *J. S. Am. Earth Sci.* 16, 649–666.
- Rammlmair, D., 1986. Chromite in Philippines: Its relationship to the tectonic setting of the host ophiolites: Examples from Zambales and Palawan, in Chromites. UNESCO's ICP-197 Project Metallogeny of Ophiolites: Athens, Greece, Theophaustus 199–228.
- Rammlmair, D., Raschka, H., Steiner, L., 1987. Systematics of chromite occurrences in Central Palawan, Philippines. *Mineral. Deposita* 22, 190–197.
- Rollinson, P., 2008. The geochemistry of mantle chromitites from the northern part of the Oman ophiolite: inferred parental melt compositions. *Contrib. Mineral. Petrol.* 156, 273–288.
- Şenel, M., Ercan, T., 2002. Geological map of Turkey (Van, Scale: 1/500,000). General Directorate of Mineral Research and Exploration No:12.
- Şengör, A.M.C., 1984. The Cimmeride orogenic system and the tectonics of Eurasia. *Geol. Soc. Am. Spec. Pap.* 195, 82.
- Şengör, A.M.C., Kidd, W.S.F., 1979. The post-collisional tectonics of the Turkish–Iranian plateau and a comparison with Tibet. *Tectonophysics* 55, 361–376.
- Şengör, A.M.C., Yılmaz, Y., 1981. Tethyan evolution of Turkey: a plate tectonic approach. *Tectonophysics* 75, 181–241.
- Şengör, A.M.C., Özären, M.S., Keskin, M., Sakınç, M., Özbakır, A.D., Kayan, İ., 2008. Eastern Turkish high plateau as a small Turkic-type orogen: implications for post-collisional crust-forming processes in Turkic-type orogens. *Earth Sci. Rev.* 90, 1–48.
- Şengör, A.M.C., Özären, S., Zor, E., Genç, T., 2003. East Anatolian high plateau as a mantlesupported, N–S shortened domal structure. *Geophys. Res. Lett.* 30, 45–80.
- Shervais, J.W., 2001. Birth, death, and resurrection: the life cycle of suprasubduction zone ophiolites. *Geochem. Geophys. Geosyst.* 2. <http://dx.doi.org/10.1029/2000GC000080>.
- Shibata, T., Thompson, G., Frey, F.A., 1979. Tholeiitic and alkali basalts from the mid-Atlantic ridge at 43°N. *Contrib. Mineral. Petrol.* 70, 127–141.
- Thayer, T.P., 1964. Principal features and origin of podiform chromite deposits and some observations on the Guleman–Soridag District. *Turk. Econ. Geol.* 59, 1497–1524.
- Thayer, T.P., 1969. Gravity differentiation and magmatic replacement of podiform chromite deposits, "magmatic ore deposits". In: Wilson, H.D.B. (Ed.), *Monograph 4 Economic Geology*, pp. 132–146.
- Tredoux, M., Lindsay, N.M., Davies, G., MacDonald, I., 1995. The fractionation of platinum-group elements in magmatic system, with the suggestion of a novel causal mechanism. *S. Afr. J. Geol.* 98, 157–167.
- Uçurum, A., Koptyagel, O., Lechner, J.P., 2006. Main-component geochemistry and platinum-group-element potential of Turkish chromite deposits, with emphasis on the Muğla area. *Int. Geol. Rev.* 48, 241–254.
- Uçurum, A., Lechner, P.J., Larson, L.T., 2000. Platinum-group element distribution in chromite ores from ophiolite complexes, western Turkey. *Trans. Inst. Min. Metall. Sect. B – Appl. Earth Sci.* 109, 112–120.
- Üşümsezoglu, Ş., 1986. A new approach to the generation of chromite bodies of Kefdağ and Soridag (Guleman). *Cumhuriyet Univ. Geol. Eng.* 29, 47–60.
- Uysal, I., Tarkian, M., Sadıkclar, M.B., Şen, C., 2007a. Platinum-group-element geochemistry and mineralogy of ophiolitic chromitites from Kop mountain, northeastern Turkey. *Can. Mineral.* 45, 355–377.
- Uysal, I., Zaccarini, F., Garuti, G., Meisel, T., Tarkian, M., Heinz Jürgen Bernhardt, J.H., Sadıkclar, M.B., 2007b. Ophiolitic chromitites from the Kahramanmaraş area, southeastern Turkey: their platinum-group elements (PGE) geochemistry mineralogy and Os-isotope signature. *Ophioliti* 32 (2), 151–161.
- Uysal, I., Sadıkclar, B., Tarkian, M., Karslı, O., Aydin, F., 2005. Mineralogy and composition of the chromitites and their platinum-group minerals from Ortaca (Muğla–SW Turkey): evidence for ophiolitic chromitite genesis. *Mineral. Petrol.* 83, 219–242.
- Uysal, I., Tarkian, M., Sadıkclar, B., Zaccarini, F., Meisel, T., Garuti, G., Heidrich, S., 2009b. Petrology of Al- and Cr-rich ophiolitic chromitites from the Muğla, SW Turkey: implications from composition of chromite, solid inclusions of platinum-group mineral, silicate, and base-metal mineral, and Os-isotope geochemistry. *Contrib. Mineral. Petrol.* <http://dx.doi.org/10.1007/s00410-009-0402-9>.
- Uysal, I., Zaccarini, F., Sadıkclar, B., Bernhardt, H.J., Bigi, S., Garuti, G., 2009a. Occurrence of rare Ru–Fe–Os–Ir–oxide and associated platinum-group minerals (PGM) in the chromitite of Muğla ophiolite SW-Turkey. *N. Jb. Mineral. (Abh.)* 185, 323–333.
- Uysal, I., Ersoy, E.Y., Karslı, O., Dilek, Y., Sadıkclar, M.B., Ottley, C.J., Tiepolo, M., Meisel, T., 2012. Coexistence of abyssal and ultra-depleted SSZ type mantle peridotites in a Neo-Tethyan Ophiolite in SW Turkey: constraints from mineral composition, whole-rock geochemistry (major–trace–REE–PGE), and Re–Os isotope systematics. *Lithos* 132–133, 50–69.
- Walker, D.A., Cameron, W.E., 1983. Boninite primary magmas: evidence from the Cape Vogel Peninsula, PNG. *Contrib. Mineral. Petrol.* 83, 150–158.
- Wilson, M., 1989. Igneous Petrogenesis: A Global Tectonic Approach. Unwin Hyman, London.
- Yaman, S., Ohnenstetter, M., 1991. Distribution of platinum-group elements of chromite deposits within ultramafic zone of Mersin ophiolite (South Turkey). *Bull. Geol. Congr. Turk.* 6, 253–261.
- Yılmaz, Y., Saroğlu, F., Güner, Y., 1987. Initiation of the neomagmatism in East Anatolia. *Tectonophysics* 134, 177–199.
- Zaccarini, F., Garuti, G., Proenza, J.A., Campos, L., Thalhammer, O.A.R., Aiglsperger, T., Lewis, J., 2011. Chromite and platinum-group-elements mineralization in the Santa Elena ophiolitic ultramafic nappe (Costa Rica): geodynamic implications. *Geol. Acta* 9 (3–4), 407–423.
- Zhou, M.F., Bai, W.-J., 1992. Chromite deposits in China and their origin. *Mineral. Deposita* 27, 192–199.
- Zhou, M.F., Robinson, P.T., 1994. High-Cr and high-Al podiform chromitites, western China: relationship to partial melting and melt/rock reaction in the upper mantle. *Int. Geol. Rev.* 36, 678–686.
- Zhou, M.F., Robinson, P.T., 1997. Origin and tectonic environment of podiform chromite deposits. *Econ. Geol.* 92, 259–262.
- Zhou, M.F., Robinson, P.T., Bai, W.-J., 1994. Formation of podiform chromitites by melt/rock interaction in the upper mantle. *Mineral. Deposita* 29, 98–101.
- Zhou, M.F., Robinson, P.T., Malpas, J., Li, Z., 1996. Podiform chromitites in the Luobusa ophiolite (southern Tibet): implications for melt–rock interaction and chromite segregation in the upper mantle. *J. Petrol.* 37, 3–21.
- Zhou, M.F., Sun, M., Keays, R.R., Kerrich, R.W., 1998. Controls on platinum group elemental distributions of podiform chromitites: a case study of high-Cr and high-Al chromitites from Chinese orogenic belts. *Geochim. Cosmochim. Acta* 62 (4), 677–688.